DTU Library

Accelerating Battery Characterization Using Neutron and Synchrotron Techniques
Toward a Multi-Modal and Multi-Scale Standardized Experimental Workflow

Atkins, Duncan; Capria, Ennio; Edström, Kristina; Famprikis, Theodosios; Grimaud, Alexis; Jacquet, Quentin; Johnson, Mark; Matic, Aleksandar; Norby, Poul; Reichert, Harald

Total number of authors:
14

Link back to DTU Orbit

Accelerating Battery Characterization Using Neutron and Synchrotron Techniques: Toward a Multi-Modal and Multi-Scale Standardized Experimental Workflow

Duncan Atkins, Ennio Capria, Kristina Edström, Theodosios Famprikis, Alexis Grimaud, Quentin Jacquet, Mark Johnson, Aleksandar Matic, Poul Norby, Harald Reichert, Jean-Pascal Rueff, Claire Villevieille, Marnix Wagemaker,* and Sandrine Lyonnard*

Li-ion batteries are the essential energy-storage building blocks of modern society. However, producing ultra-high electrochemical performance in safe and sustainable batteries for example, e-mobility, and portable and stationary applications, demands overcoming major technological challenges. Materials engineering and new chemistries are key aspects to achieving this objective, intimately linked to the use of advanced characterization techniques. In particular, operando investigations are currently attracting enormous interest. Synchrotron- and neutron-based bulk techniques are increasingly employed as they provide unique insights into the chemical, morphological, and structural changes inside electrodes and electrolytes across multiple length scales with high time/spatial resolutions. However, data acquisition, data analysis, and scientific outcomes must be accelerated to increase the overall benefits to the academic and industrial communities, requiring a paradigm shift beyond traditional single-shot, sophisticated experiments. Here a multi-scale and multi-technique integrated workflow is presented to enhance bulk characterization, based on standardized and automated data acquisition and analysis for high-throughput and high-fidelity experiments, the optimization of versatile and tunable cells, as well as multi-modal correlative characterization. Furthermore, new mechanisms, methods and organizations such as artificial intelligence-aided modeling-driven strategies, coordinated beamtime allocations, and community-unified infrastructures are discussed in order to highlight perspectives in battery research at large scale facilities.

1. Introduction

Batteries have enabled the recent mobile electronic consumer revolution and are now also at the heart of the electrical transport transition and increasingly used to provide short term energy reserves to stabilize electrical grids – notably for renewable energy sources with their intrinsic, intermittent nature. This has driven the actual exponential demand for batteries, not only in amounts/volume, but also for improved electrochemical performance parameters and safety criteria. At the same time, new battery designs, often relying also on new chemistries, are required to meet environmental/societal boundary conditions such as the use of abundant elements that can be readily mined, processed, and recycled, all with a low ecological footprint.

To tackle these challenges and meet this tremendous demand for better batteries, it is crucial to accelerate materials discovery, in parallel with the automation of all aspects of battery design. Developing the in-depth understanding of the electrochemical processes that dictate battery

D. Atkins, M. Johnson
Institut Laue-Langevin (ILL)
BP 156, 71 Avenue des Martyrs, Grenoble 38042, France
E. Capria, H. Reichert
European Synchrotron Radiation Facility (ESRF)
CS 40220, 71 Avenue des Martyrs, Grenoble 38043, France
K. Edström
Department of Chemistry – Ångström Laboratory
Uppsala University
Box 538, Uppsala S-751 21, Sweden

The ORCID identification number(s) for the author(s) of this article can be found under https://doi.org/10.1002/aenm.202102694.

[+]Present address: Université Grenoble Alpes, Université Savoie Mont Blanc, CNRS, Grenoble INP, LEPMI, Grenoble 38000, France

T. Famprikis, M. Wagemaker
Department of Radiation Science and Technology
Delft University of Technology
Mekelweg 15, Delft 2629JB, The Netherlands
E-mail: M.Wagemaker@tudelft.nl
A. Grimaud
Chimie du Solide et de l'Energie
Collège de France
UMR 8260, Paris 75231 Cedex 05, France
A. Grimaud
Réseau sur le Stockage Electrochimique de l'Energie (RS2E)
CNRS FR 3459, 33 rue Saint Leu, Amiens Cedex 80039, France
Q. Jacquet, C. Villevieille,[+] S. Lyonnard
Université Grenoble Alpes
IRIG-SyMMES
CEA
CNRS
Grenoble 38000, France
E-mail: Sandrine.lyonnard@cea.fr

performance requires new methodologies to characterize battery materials and the key processes at play during a battery's lifecycle.

Over the past three decades, active materials have generally been examined ex situ and/or post mortem involving the development of an array of advanced characterization techniques.[1,2] More recently, the advent of operando characterization methods monitoring the behavior of batteries under real working conditions has provided unprecedented opportunities to explore the variety of inter-related multi-scale, multi-reactions processes involving chemical, structural and morphological changes during battery operation. However, investigating electroactive materials and their properties inside operating batteries is extremely complex for several reasons: i) the number of elements involved, which complicates processes deconvolution, ii) the extended range of time and length-scales to be considered, starting from the atomic scale and ending with complete cells, iii) the sensitivity of cell components to air/moisture, the necessity to eliminate external contamination, and having to traverse the cell's outer casing, which limit the methods available and may influence data collection.

Lab-scale techniques are being constantly developed to measure structural, morphological, and chemical changes at nm, μm, or mm scales during battery cycling, for example, operando transmission electron microscopy,[3] nuclear magnetic resonance (NMR),[4] Fourier transform infra-red,[5] Raman,[6] and more. To complement lab-scale studies, cutting-edge experiments at large scale facilities (LSF) have been increasingly developed. Synchrotron and neutron techniques are tools of choice because both high energy X-rays and neutrons deeply penetrate matter, allowing materials in realistic cell designs, as well as in fully commercial devices, to be thoroughly probed with complementary chemical sensitivity and sufficient spatio-temporal resolutions to monitor the multiple changes during operation and cycling. Experimental advances have included the availability of bespoke cells for spectroscopy, diffraction, scattering and 2D/3D imaging studies, accompanied by major progress in big-data analysis, particularly important in tomography studies. Indeed, such continuous improvements in experimental techniques, notably in terms of time-resolution, must be complemented by correspondingly rapid neutron/synchrotron data acquisition and analysis protocols, in order to be useful to the battery community.

In this paper, we provide our vision on the current role and future prospects of synchrotron-based X-ray and neutron-based techniques as applied to batteries, specifically for monitoring relevant bulk processes in operando mode. We expressly spotlight bulk-type techniques since a parallel paper focuses on surface and interface characterizations.[7] We address the types of bulk processes involved and their relation to battery electrochemical performance, the progress made in X-ray and neutron techniques for bulk characterization, and the need for standardization and multi-method approaches coupled with operando/in situ electrochemical cell development. Also, we introduce future automated, standardized, experimental workflows, incorporating multi-probe characterization, real-time feed-back loops with numerical modeling, machine/deep learning (ML/DL) and artificial intelligence (AI), and correlative data analysis. Lastly, we discuss our visions and perspectives toward interoperable infrastructures and new LSF-connected research hubs, all aimed at improving our fundamental understanding and ultimately enabling a paradigm shift in design and characterization methodology for next generation batteries.

2. Key Bulk Processes in Batteries

In rechargeable batteries, energy is stored through a chemical process, which is then converted to electrical energy upon discharge, and vice-versa upon charging. This is mediated by mobile ions (e.g., Li^+, Na^+) that can shuttle between the two electrodes, through an ion conducting and electrically insulating electrolyte. The negative and positive electrode materials are designed to host lithium ions, for instance by atomic voids in the crystal lattice, and provide the charge compensating electrons by a redox couple, for example, Co^{3+}/Co^{4+} in Li_xCoO_2. This ability is quantified by the specific capacity which, in combination with the battery voltage, determines the energy density of the cell. Electrode materials can store mobile ions. (De)lithiation causes changes in both the electronic and atomic structures of the electrode materials, which in turn influences the kinetics of both ions and electrons. The atomic-scale processes can induce mesoscopic and macroscopic modifications in morphology, affecting overall electrode properties and ultimately their electrochemical performance. This is further complicated by the number of aging mechanisms which impact the battery life cycle, its specific capacity, rate capability, energy, and power density.

These basic considerations aid in identifying several inter-related bulk processes, to be distinguished from interface processes, the monitoring of which would allow a deconvolution of bulk and interface mechanisms and battery performance. These include:

1) Structural/phase changes (atomic-scale up to single crystallites), affecting the intrinsic charge–carrier conductivity (electron and ion) and (heterogeneous) electrode morphology (nm scale up to complete electrodes),
2) The associated redox valence changes,
3) Inhomogeneities in the structure/phase and redox valence changes over the electrode volume (nm scale up to complete electrodes).

These bulk processes are summarized in **Figure 1**, where the length-scales involved are schematically represented, that

A. Matic
Department of Physics
Chalmers University of Technology
Göteborg 41296, Sweden

P. Norby
DTU Energy
Technical University of Denmark
Kgs. Lyngby 2800, Denmark

J.-P. Rueff
Synchrotron SOLEIL
L'Orme des Merisiers
BP 48 Saint-Aubin, Gif-sur-Yvette 91192, France

J.-P. Rueff
Sorbonne Université
CNRS
Laboratoire de Chimie Physique-Matière et Rayonnement
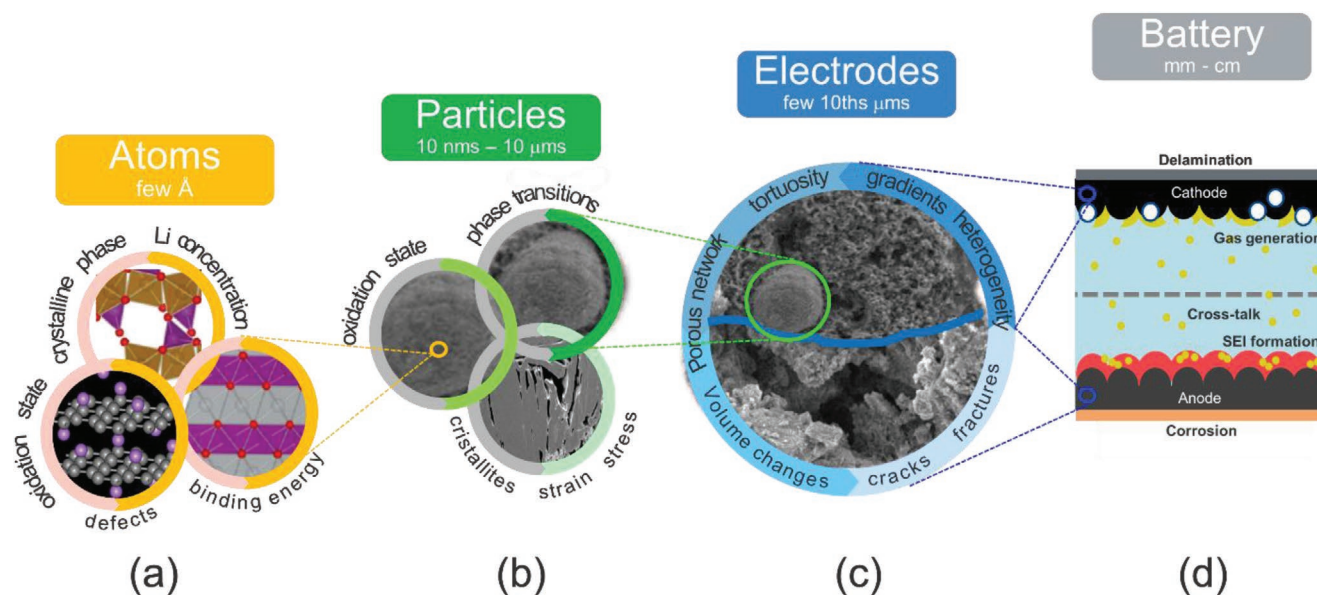Paris 75005, France

Figure 1. Key bulk processes happening in batteries at the various length scales, from a) atoms to b) individual active particles, c) electrodes/electrolytes layers, and d) up to full battery devices.

is, atomic (below the nanometer, Figure 1a), particle (few nm up to tens of microns, Figure 1b), electrode (up to 100 microns, Figure 1c) and device scale (mm to cm, Figure 1d). In the following, we give a short overview of each of these aspects before describing advanced techniques used to characterize batteries throughout the spatial ranges involved.

1) We can distinguish several types of Li reactions that can induce structural changes on the atomic scale in battery electrode materials: insertion reactions[8] (or intercalation if the electrode has a layered structure such as graphite and $LiCoO_2$), conversion reactions, alloying reactions,[9] and deposition or growth reactions (for example of Li metal anodes[10] or of Li_2O_2 oxygen cathodes[11,12]). Insertion and alloying electrodes can display a solid solution behavior characterized by a gradual change in composition, a first order phase transition, or combinations of both. The gradual evolution of the lithium concentration during solid solution reactions corresponds to a gradual change in voltage, whereas the constant electrochemical potential during first order phase transitions results in a potential plateau.[13] For conversion reactions, the involved processes are more complicated because in this case, the ternary phase diagram allows concurrent first order and solid solution transformations.[13]

   The phase transition mechanisms can have large impact on battery performance in various ways. For instance, during first order transitions, coherent phase interfaces form, which may result in internal stress, as is often observed for insertion reactions. This in turn may affect the Li chemical potential, phase stability and transformation kinetics, and has been shown to play a role in the ≈7% volumetric change for $LiFePO_4$ cathodes upon (de)lithiation.[14] For sufficiently large volumetric changes, strain release may lead to the irreversible formation of dislocations and cracks at particle and electrode scales, which leads to mechanical failure of the electrode, and

intrinsic modifications in charge transport properties and electronic conductivity through band structure evolution.[15] Furthermore, the formation of cracks within a particle can isolate active material from the charge transport network, effectively lowering the battery specific capacity. A well-known example where large volumetric changes represent the main challenge toward achieving a high degree of reversibility (and thus commercialization) is the Si anode which undergoes a 300% volume expansion in the bulk. The most extreme case of electrode volumetric changes are deposition and growth reactions, where the electrode is deposited from solvated species, forming a specific morphology. This morphology is dictated by the phase, the rugosity of the surface, and surface stability of the deposited product, the electrolyte reactions and the (local) deposition rate, where the latter depends on the (dis)charge current and intrinsic morphology. Intensively studied examples include Li-metal anodes[10] and Li_2O_2 (Li-oxygen) cathodes,[11] where the morphology is decisive in the reversibility of the charge storage. Also, one could include the solid electrolyte interphase (SEI) formation, which plays a key role in reversibility and the cycle life of a battery.[16] Although typically qualified as an interfacial region, the thickness/volume of the SEI layer may reach dimensions approaching the bulk, that is, > 10 nm. The SEI will not be described further in this paper as we focus exclusively on bulk-type processes. An overview of surface/interface reactions and relevant characterization techniques can be found in ref. [7].

2) Reversible (de)lithiation of electrode materials gives rise to a redox reaction of the electrode material, driven by the ready tendency for Li to donate its 2s electron (small electronegativity) to the neighboring environment. Either the Fermi level in the itinerant electron band (e.g., for graphite electrodes) or a transition metal provides the redox couple, which determines the energy and thus the potential of the electrode in question. The potential of a redox couple is not only determined by

ADVANCED
SCIENCE NEWS

www.advancedsciencenews.com

ADVANCED
ENERGY
MATERIALS

www.advenergymat.de

the formal valence state but also by the nearest bonding element, and therefore the structure and character of the atoms in the material.[17] In contrast to this reversible redox state, irreversible redox changes may induce deactivation of electrode species, for instance through oxygen release, changes in oxidation state of transition metal species that lead to dissolution in the electrolyte, and irreversible phase transitions consuming Li. Another category of irreversible redox reactions is SEI formation, where solvent and/or solvated species are redox active leading to irreversible Li loss and to deactivation of electrode material. As discussed above, these irreversible processes are responsible for reducing battery life, as well as lowering cell performance.

3) Inhomogeneities in phase transitions and redox reactions throughout the electrode material occur at different length scales: from nm in individual electrode particles (Figure 1b), progressing up to the dimensions of complete composite electrodes (hundreds of μm) as shown in Figure 1c. On the electrode crystallite or particle level, inhomogeneities in charge storage can arise through the phase transformation mechanism, the surface/interface structure (i.e., facet termination and grain boundaries), and structural defects. As described in (1), inhomogeneities at the crystallite level can induce cracks, deactivating part of the active material which in turn lowers the battery capacity. Inhomogeneities on larger length scales, such as agglomerates of crystallites up to the porous morphology of complete electrodes and whole batteries, can have a thermodynamic origin or can be induced by charge transportation (electron and ion) limitations under non-equilibrium (dis)charge conditions. The latter are determined by intrinsic material properties and the porous morphology, that is, by the porosity, tortuosity, and conductivity of the components. Thermodynamic origins of intra-particle inhomogeneities include a difference in insertion potential due to a distribution of nanoparticle sizes[18] when combining different electrode materials,[19] or the nature of the phase transition. For example, the particle-by-particle transformation mechanism in $LiFePO_4$ has been associated with hysteresis[20] and has been suggested to give rise to a memory effect that can influence the observed potential.[21] The kinetic origin of inhomogeneities stems from charge transport limitations, which in turn are generally determined by the electrode morphology (including electrode thickness, porosity, and tortuosity).[19,22,23] An important implication of inhomogeneous charge storage distributions is that this may lead to the localization of current and overpotential in areas of the electrode which may in turn induce accelerated irreversible reactions such as cracks and SEI formation, as described above. These are responsible for the degradation of battery performance parameters such as specific capacity, energy density, rate capability, and cycle life.

An in-depth understanding of such a variety of inter-related processes requires their monitoring under operando conditions, that is, the data collection on single cell is acquired during continual (dis)charge. Moreover, the extended range of length-scales involved (Figure 1) calls for the development of tools capable of detecting key mechanisms at the appropriate scales, but also strategies to bridge these various scales

to obtain a continuous description of processes during battery operation. This sets the stage for synchrotron X-ray and neutron techniques applied to batteries which can eliminate classical experimental limitations and ultimately enable to establish the direct relationship between bulk electrode/electrolyte properties and battery performance.

3. Neutron and Synchrotron Bulk Characterization Techniques

3.1. A Rich Landscape of Techniques

The upgrade of sources, optics, detection systems, as well as the continuous improvement of ultra-specialized instruments and beamlines at LSF, has allowed significant advances in battery operando characterization by pushing experimental limits in terms of sensitivity and resolution. An array of instruments is available at synchrotron and neutron facilities, each being optimized in general to monitor one or two key characterizations. Diffraction and scattering techniques are employed to observe the atomic ordering/crystal/nanoscale structure;[24] spectroscopy techniques allow us to observe the redox valence changes, local dynamics and local structure; and imaging and tomography techniques probe inhomogeneities and/or distributions of density, redox valence, and mesoscale structures.

Synchrotron techniques (**Figure 2**) can provide time-resolved data with high spatial resolutions, chemical sensitivity, 2D/3D spatially resolved structural maps, and volume reconstructions. X-ray diffraction (XRD),[25] absorption spectroscopy (XAS),[26] photoelectron spectroscopy (XPS),[27] and tomography (XRT)[28] have proven to be amongst the workhorse characterization techniques for battery materials and devices, while small angle X-ray scattering (SAXS),[29] resonant inelastic X-ray scattering (RIXS),[30] scanning transmission X-ray microscopy (STXM),[31] X-rays reflectivity (XRR),[32] and X-ray Raman scattering (XRS)[33] have recently been added to the battery researcher's toolbox and as such have yet to provide their full potential. Spatially resolved techniques, including ultimate nanoscale resolution X-ray tomography,[34] are nowadays becoming increasingly popular. However, several challenges must be addressed for their application in operando mode, particularly the extraction of relevant information from the large volume of data generated and the design of adapted cells allowing nanoscale resolution. Neutron techniques (**Figure 3**) generally have lower time resolutions, but they have crucial advantages, for example, neutrons are less intrusive than high-energy X-rays and isotopic exchange can be used to tag elements or achieve contrast match conditions. For instance, ^6Li and ^7Li have significantly distinct neutron absorption cross-sections, permitting their differentiation, whereas this is impossible with X-rays. Similarly, $^1H/^2D$ isotopic exchange can be used, as hydrogen is often present in batteries (electrolyte/separator/binder).[35] Neutron powder diffraction (NPD) has a long and successful track record in battery characterization, although great care must be taken in cell design to optimize signal-to-noise ratio.[36] Small angle neutron scattering (SANS),[35] neutron reflectometry (NR),[37] neutron imaging/computed tomography (NI and NCT),[38,39] and neutron depth profiling (NDP)[23,40] have all been successfully
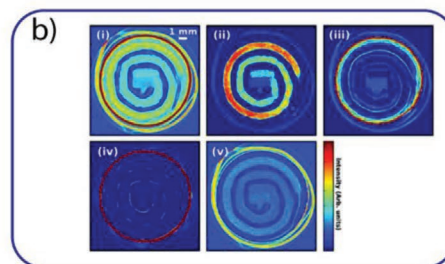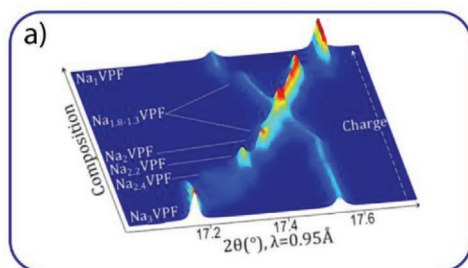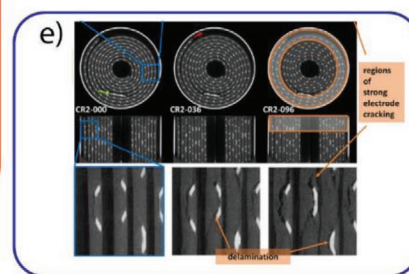
Figure 2. Chart comparing the length scale probed by several synchrotron techniques, the dimensionality of the probed properties in the electrode/battery, and to what extent the operando cells compare to commercial or lab cells. Examples of a) X-ray diffraction (XRD). Reproduced with permission.[42] Copyright 2021, American Chemical Society. b) Scattering computed tomography. Reproduced according to the terms of the CC-BY license.[43] Copyright 2015, The Authors. c) X-ray absorption spectroscopy (XAS). Reproduced with permission.[44] Copyright 2021, American Chemical Society. d) X-ray photoelectron spectroscopy (XPS). Reproduced according to the terms of the CC-BY license.[45] Copyright 2016, The Authors, and e) microtomography (XCT). Reproduced according to the terms of the CC-BY license.[38] Copyright 2020, The Authors. Datasets are shown. The x-axis shows the typical length scale probed (Å, nm, µm), whereas the y-axis indicates the possibility to achieve 1D, 2D, or 3D property mapping, respectively. In this representation, a 1D property or parameter is typically a mean value averaged over the volume of the probed material, while 2D indicates the possibility to scan across the thickness of a material and spatially resolve the property distribution along one dimension. 3D indicates that the full volume (zone of interest) is resolved and voxel-type information is obtained. Moreover, the colors indicate to what extent the specific existing cells represent realistic (i.e., electrochemical performance is comparable to commercial cells, blue) and/or commercial cells, as opposed to model cell designs (orange), and whether operando mode is available (green contour).

applied to provide structural information on battery materials, Li concentration gradients, and SEI growth mechanism, with yet further developments proposed in order to shed light on as yet inaccessible degradation mechanisms. Quasi-elastic neutron scattering (QENS) is unique in providing a direct observation of ionic conduction mechanism on timescales ranging from picoseconds through to microseconds, yielding key information on the geometrical character of the ionic motion, distinguishing for example between continuous, liquid-like diffusion, and discrete hopping between specific sites.[41]
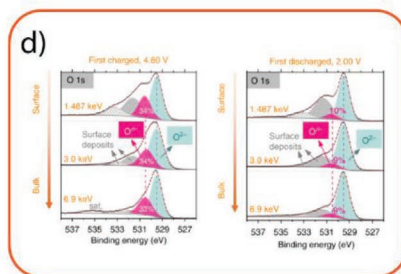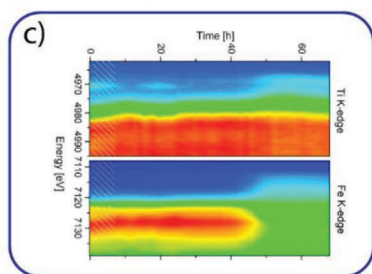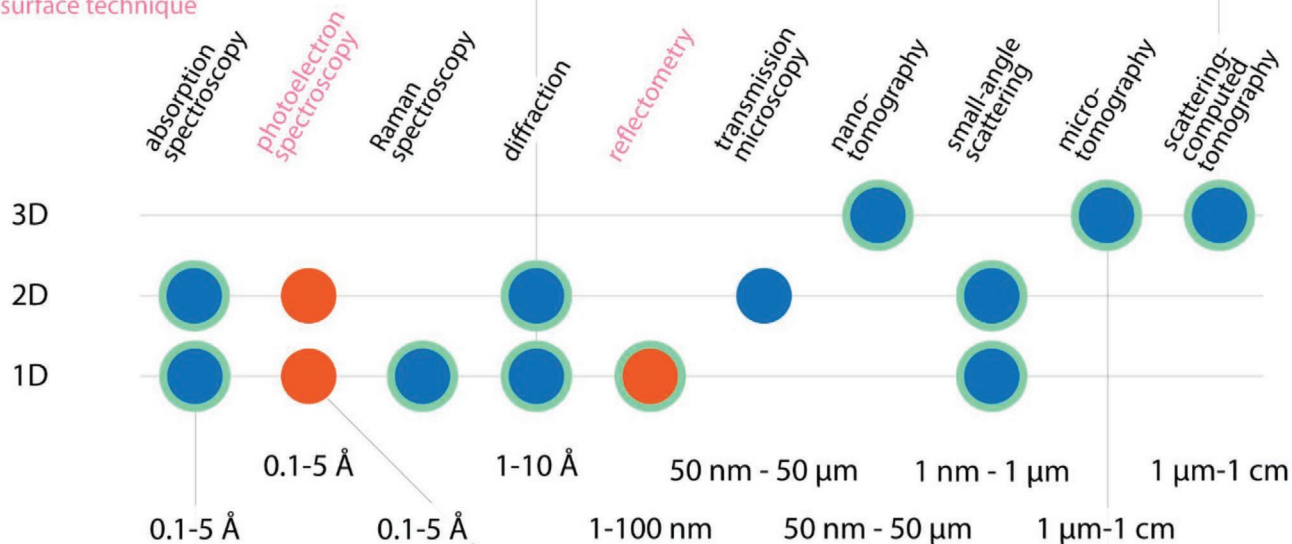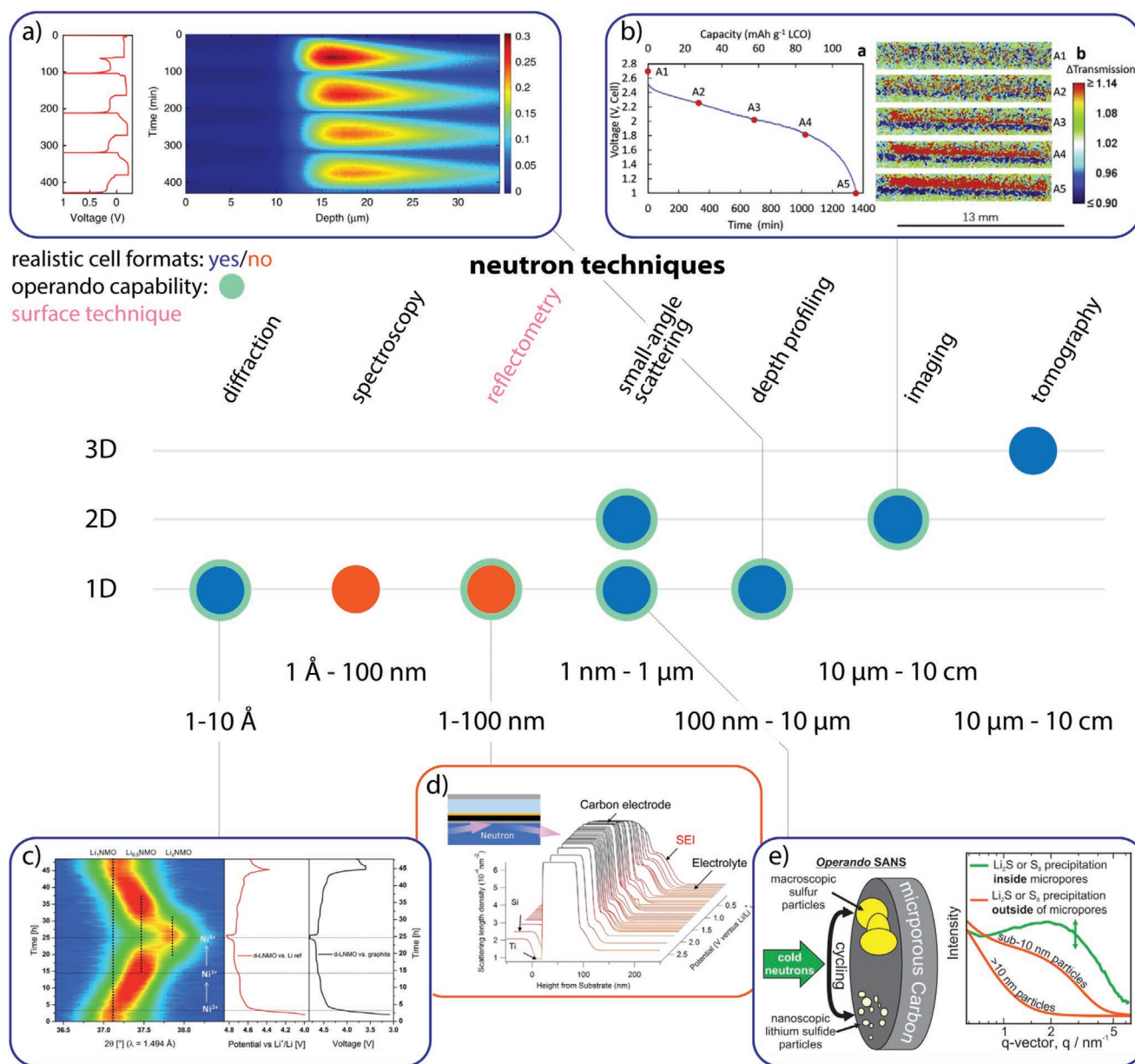
Figure 3. Chart comparing the length scale probed by several neutron techniques, the dimensionality of the probed properties in the electrode/battery, and to what extent the operando cells compare to commercial or lab cells. Examples of a) neutron depth profiling (NDP). Reproduced according to the terms of the CC-BY license.[46] Copyright 2018, The Authors. b) imaging (NI). Reprinted with permission.[47] Copyright 2019, Elsevier. c) Powder diffraction (NPD). Reproduced with permission.[48] Copyright 2017, Royal Society of Chemistry. d) reflectometry (NR). Reproduced with permission.[49] Copyright 2021, American Chemical Society. e) Small angle scattering (SANS). Reproduced with permission.[50] Copyright 2021, American Chemical Society.

Several exhaustive reviews provide a detailed overview of the characteristics of LSF techniques and their use in battery research.[2,51] In the forthcoming sections, we highlight the benefits and challenges associated with the development of some recent techniques to complete and extend the usual battery characterization portfolio, with focus on "bulk" investigation. It should be noted that the assignment to surface and/or bulk techniques is sometimes ambiguous, as it is not trivial to quantify the appropriate length scale from where bulk processes stop and interface/surface processes start, for example, SEI formation and growth. Accordingly, techniques such as

neutron reflectometry, X-rays reflectivity, and XPS cover length scales that cross the boundary between interface and bulk. These specific techniques are covered in a parallel review on interface processes[7] and therefore will not be discussed here.

3.2. Small Angle Scattering Techniques

Small angle neutron and X-ray scattering (SANS and SAXS) probes the meso and micro-structure (typically 1–300 nm) of materials and cell components. This gives access to several

**ADVANCED
SCIENCE NEWS**

www.advancedsciencenews.com

**ADVANCED
ENERGY
MATERIALS**

www.advenergymat.de

important properties of the materials under investigation, for example, particle sizes and shapes, the presence of agglomerates and nanostructured domains, or solvation structures, as well as the morphological parameters of electrodes (pore size and shape) and the presence of interfaces. For instance, SAXS was used to probe the morphological evolution in composite anodes, such as Si/C anodes where morphological changes of the silicon phase on 10–20 nm length scales can be directly monitored during cell lithiation/delithiation and correlated to the loss of capacity after long-term cycling.[52,53] The formation of nanopores in Li-rich NMC cathodes was also evidenced by ex situ SAXS, and assigned to a structural consequence of oxidation.[54] SAXS is also very useful to probe the structure of electrolytes beyond nearest neighbor correlations as it provides information on solvation structures (on few nm length scale) as a function of carbonate based solvent[55] or as a function of salt concentration in highly concentrated electrolytes.[56] SANS, on the other hand, offers the possibility of measuring light elements such as Li or H in commercial cells due to the low absorption of neutrons from cell casing. As an example, a full NMC/graphite pouch cell was investigated operando by SANS with an integration time ≈10 min, giving novel insights into the lithiation process of graphite particles.[57] Pore clogging/filling by SEI products was also measured by operando SANS on silicon–graphite composite anodes.[35] The interfaces in LTO electrodes were probed by SANS, where size-dependent pore filling kinetics was followed operando suggesting the presence of SEI.[58] Also, the impact of high electrolyte concentration on electrochemical reactions was investigated in half-cells on Li/ordered mesoporous carbon electrodes, using SANS to probe pore filling and carbon framework expansion.[58]

Beyond Li-ion technology, SANS and SAXS are considered key techniques for next generation batteries featuring mesostructured electrode materials (hard carbon for Na-ion batteries,[59] or carbon composites for Li–O₂ and Li-sulfur cells[47,50]) or mesostructured solid electrolytes (polymers,[60] ceramics or composite/hybrid membranes).

With the development of third and recently fourth generation synchrotron sources, SAXS now offers excellent temporal and spatial resolution. Sub-second integration times enable studies of fast kinetic processes as well as operando studies at high charge/discharge rates (>1C), whereas micrometer beams enable scanning experiments and even tomographic studies of heterogenous or hierarchical materials. SANS is currently limited to integration times in the order of minutes, and a high flux of cold neutrons is required for rapid acquisitions enabling operando experiments at high charge/discharge rates, but the upgrade of existing facilities and the advent of new spallation sources open exciting vistas for battery research with neutrons.

A major challenge regarding these techniques is the development of SANS/SAXS compatible cells enabling i) to extract the signal only from the desired cell component, that is, avoiding the usual transmission geometry, ii) to perform 2D/3D spatially-resolved operando nanostructural mappings, iii) to perform combined SANS and SAXS investigations, and iv) to measure long-term ageing to ensure a better understanding of failure mechanisms. The juxtaposition of SANS with a laboratory X-ray set-up was made available recently at the ILL on the

D22 spectrometer,[61] which should in principle allow simultaneous SANS/SAXS measurements by using a multi-modal cell.

3.3. Spatially-Resolved Techniques

Spatially resolved structural and microstructural information from in situ and operando experiments on battery electrodes during (dis)charge is becoming increasingly important for i) understanding the reaction mechanisms at early charging stages to understand the role of the "activation" or "formation" cycle (stable SEI obtained through a specific electrochemical protocol/temperature) and ii) the long term cycling processes or ageing mechanisms that help improve battery chemistry in rechargeable batteries.

Spatially resolved operando diffraction experiments are crucial to studying structural evolutions such as homogeneity and phase distribution in battery electrodes during operation,for example, phase redistribution in zinc–air batteries,[62] lithiation heterogeneities in graphite,[25] and silicon-graphite,[63] long-term cycling stability of high voltage spinel cathode versus graphite,[48,64] degradation mechanisms in Li–S batteries up to 35 cycles,[65] or NPD mappings.[66,67] Computed tomography (CT) methods are able to describe the macrostructure, interconnectivity, and electronic percolation in the electrodes with a spatial resolution from <100 nm to several micrometers.[68] The contrast in CT is obtained through absorption, phase shift or scattering methods, giving access to the crystal/nano structure (XRD-CT, SAXS-CT), oxidation state, and lithium-ion bulk migration (NI, NCT), depending on the experimental methods employed.[66,69] μCT and nanoCT techniques provide invaluable insights into the mechanical and morphological degradation of electrodes, both of which play key roles in the performance decay for in state-of-the art lithium ion batteries as well as next generation technologies, for example, all-solid-state,[70,71] M-ion,[28,72] Li–O₂[73,74] and Li–S batteries.[75] For instance, Na electrodeposits were observed in solid state batteries by μCT and found to increase interfacial resistance and hinder ion diffusion, resulting in performance decay.[71] In the following, we will discuss in more detail two challenges related to spatially resolved techniques – probing individual particles and lithium distribution, respectively.

3.3.1. Challenge 1: Probing Individual Particles

To investigate changes inside individual crystallites in order to observe, for instance, domain formation and localized (de)lithiation reactions[76,77] in real time, significantly better spatial resolution is needed, for example, by using X-ray ptychography methods, where resolutions down to tens of nm are possible for model samples.[78] The experimental duration for ptychography measurements is presently measured in hours, which will need to be decreased significantly to follow processes in real time. Another limitation for nano-tomography/ptychography/computed tomography experiments is the sample size, which must be relatively small (i.e., 10–20 micrometers for ptychography) to ensure best resolutions.[79] Thus, advanced specimen preparation techniques are needed to fabricate a fully functioning device with the dimensions required.

**ADVANCED
SCIENCE NEWS**
www.advancedsciencenews.com

**ADVANCED
ENERGY
MATERIALS**
www.advenergymat.de

Operando microbeam diffraction experiments involving single or several (in the order of 100) crystallites provide local information about phase transitions and transformation of domains in the individual crystallites, therefore helping to solve questions about thermodynamics/kinetics (including the distribution of activity), domain formation, and interface stoichiometry.[77,80] The experiments, with a time scale of ≈30 s, are performed for pouch cell geometries, where grain mapping provides the possibility to determine the position of the grain in the electrode. Domain structure, strain, and stoichiometry gradients inside single crystallites can also be studied ex situ/in situ/operando using coherent X-ray diffraction imaging (CXDI) of single crystallites[81] and scanning X-ray microscopy.[82]

3.3.2. Challenge 2: Probing Lithium Distribution

Spatially-resolved neutron techniques provide valuable snapshots of lithium distribution/concentration during the battery's life-cycle, and often for commercial batteries. Advanced, multi-modal (coupled neutron and X-ray) 3D imaging techniques have recently been used to obtain bulk information during battery operation for both the Li-rich components (Li-migration in electrode/electrolyte) using n-data, and metallic battery component meso-scale evolutions obtained from an integrated laboratory XCT set-up, with comparable spatial/temporal resolutions.[38] Degradation and failure mechanisms of a lithium–oxygen battery were also investigated by complementary neutron and X-ray tomography, enabling correlations between the morphological evolution of the Li anode and the overall cell electrochemical performance.[74] It was found that the Li anode can chemically deteriorate and irreversibly transform into a porous-structuralized transition layer, a process that continuously develops during battery operation both in charge and discharge, consuming cell components and also causing detrimental change damage to the cathode. Upgrading existing instrumentation such as the neutron and X-ray imaging instrument NeXT at the ILL, to maximize flux at the sample whilst proposing an interchangeable suite of multi-technique modes, promises to open further routes for battery research and development (R&D).

Neutron depth profiling (NDP) and neutron laminography complement NI/NCT capabilities. NDP allows accessing the Li-density concentration profile as a function of depth into the electrode and to monitor quantitatively the Li-storage (in) activity and mesoscopic Li-ion diffusion; proving insights into degradation mechanism and charge transport limitations. NDP is based on the capture reaction of cold/thermal neutrons with ^6Li (7.5% natural abundance), producing two charged particles (^4He and ^3H) with well-defined energies. By measuring the energy loss of these particles with a detector positioned perpendicular to the electrode surface, the depth-resolved Li-density concentration profile can be reconstructed (when the density of the species encountered by the charged particles is known) and averaged over the electrode surface area. In situ NDP was first applied in micro-batteries[83] and later in situ and operando to modified pouch and coin cell batteries.[40,46,84] In the latter case, the ^3H particle has a sufficiently large penetration length, allowing roughly a maximum penetration into the battery of 40 micrometers (depending on the electrode/electrolyte materials and including the current collector). The practical depth resolution is in the order of 100 nm and measurement times vary from 1 to 30 min depending on the ^6Li concentration, electrode area probed, and neutron beam characteristics.

Of course, applying neutron/X-ray characterization techniques to commercial cells, for example, pouch cell configurations or cylindrical ones, would be ideal but is far from trivial. An example of a particularly interesting development is neutron and X-ray laminography,[85] where an extended planar object can be imaged at high resolution. While the technique offers large fields of view on an extended sample at high spatial resolutions, the integration time is currently not compatible with operando studies. With the future development of laminography instrumentation and new, extremely brilliant, pulsed neutron sources like the European Spallation Source, one can envisage rapid advances in this domain.

4. Current Limitations: Beyond the Single-Shot Experiment

4.1. Isolated Datasets and Fragmented Knowledge

Investigations performed at LSF have already produced a colossal amount of data in the field of battery, as illustrated in **Figure 4** where a selection of recent synchrotron investigations of silicon-based anodes is presented. In this family of materials (including nanostructured silicon, SiO_x, Si/C composites, etc.), the alloying lithiation process induces large volume expansions and the continuous formation of the SEI, which results in morphological ageing at the level of particles and electrodes after long-term cycling. XRD was used to evaluate the strain in crystalline particles and characterize the core-shell mechanism during initial battery cycling (Figure 4a).[86] Combined, operando SAXS/WAXS was applied to investigate the sequential lithiation mechanism in graphite-silicon composites (Figure 4g), the correlation between dimensional changes of silicon in the Si-$FeSi_2$ phase, and electrochemical performance during initial cycles, as well as their evolution after more than 300 cycles.[52] Ex situ microtomography (XCT) revealed the evolutions of the porous network and phase distributions after long-term cycling on the same Si-$FeSi_2$/C composite (Figure 4f).[87] In particular, it was shown that the electrochemical performance of Li-ion batteries does not only depend on the active material used, but also on the internal architecture (i.e. the proximity of active materials such as pore networks). Similarly, operando XRD-CT (Figure 4b) was applied to quantify crystallographic heterogeneities in silicon-graphite composite electrodes with a spatial resolution of 1 mm,[63] revealing local charge transfer mechanisms by segmenting and analyzing core and shell patterns at sub-particle level. Phase distribution maps of graphite, crystalline silicon, and lithium silicides were obtained, showing spatial heterogeneities responsible from under-utilization of the electrode specific capacity. At even higher space resolutions, ex situ nanoscale tomographic imaging and in situ nanoholotomography were employed to probe the binder-particle interfaces and SEI,[88] as well as the formation of cracks and delamination.[34] In ref. [88], high-resolution ptychographic X-ray computed tomography (Figure 4c) was combined with lower resolution but higher
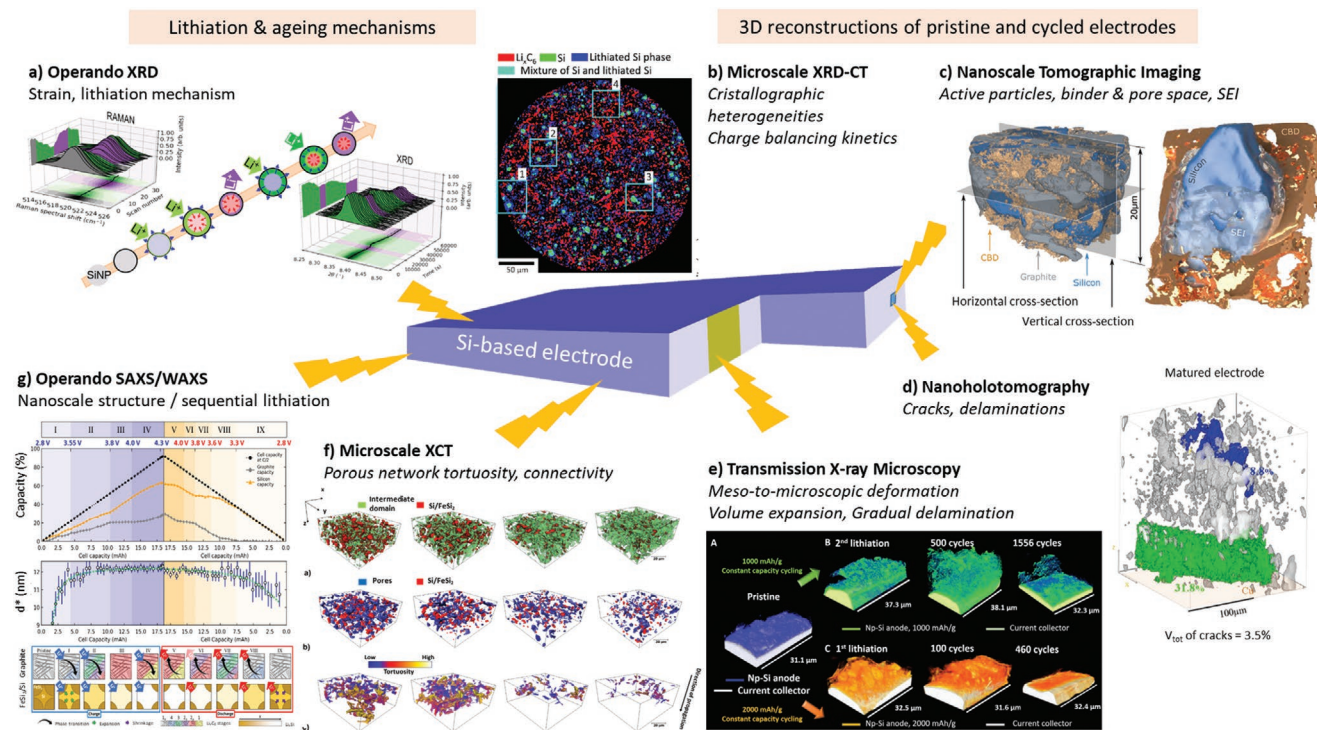
**ADVANCED
SCIENCE NEWS**

www.advancedsciencenews.com

**ADVANCED
ENERGY
MATERIALS**

www.advenergymat.de

Figure 4. Example of synchrotron characterizations on silicon-based electrodes. a) Operando XRD. Reproduced with permission.[86] Copyright 2021, American Chemical Society. b) Microscale XRD-CT. Reproduced with permission.[63] Copyright 2021, American Chemical Society. c) Nanoscale tomographic imaging. Reproduced with permission.[88] Copyright 2020, John Wiley and Sons. d) In situ nano holotomography. Reproduced with permission.[34] Copyright 2019, John Wiley and Sons. e) Transmission X-ray microscopy. Reproduced with permission.[89] Copyright 2018, Elsevier. f) Microscale XCT. Reproduced according to the terms of the CC-BY license.[87] Copyright 2020, The Authors. g) Operando SAXS/WAXS. Reproduced with permission.[52] Copyright 2021, American Chemical Society.

contrast transmission X-ray tomographic microscopy to enable the detailed, quantitative analysis of particles surface, thus revealing the amount and localization of carbon black binder and SEI coverage; critical information in understanding and modelling the electrochemical behavior of single particles within their adjacent environment. In ref. [34], a postprocessing maturation treatment of silicon anodes was shown to i) limit the expansion/contraction of the electrode and thus macro-cracks formation, ii) prevent delamination from the current collector and iii) constrain the displacement of the Si particles during charge and discharge - therefore linking the enhanced electrochemical performance of the matured electrodes to miti-gated morphological changes (Figure 4d).

Individually, these techniques provide invaluable, unique datasets, all of which are necessary to understand the correlations between silicon-based anodes design, durability, cycla-bility, and microscopic-scale features. However, it is almost impossible to post-process the gathered knowledge and inte-grate all observed phenomena into a full, consistent, multi-scale picture. Experiments are often performed by different groups, using a range of probes/cells at several beamlines under var-ying conditions, consequently making any comparison/cor-relation extremely challenging and ultimately only providing fragmented knowledge. Hence, in the absence of standardization (materials, cells, protocols, etc.), single-shot experiments may only satisfy specific short-term objectives, underscoring the need for a more holistic approach in the near-future to sup-port the rapid development of an advanced battery technology.

4.2. Actual Trends Beyond Single-Shot Experiment Workflows

Battery experiments performed at LSF usually require access to a dedicated beamline/instrument to probe one (or occasionally sev-eral) parameters of specific interest. Research is conducted using standard access modes based on proposal submission where single-shot experiments are the general rule, hence producing high-quality data focalized on one specific sample environment and targeting a specific scientific question at a given length scale (atomic, particle, electrode, or full device). The single-technique experimental workflow (**Figure 5**a) usually involves several stages extending over a significant period of time, from the nucleating idea to proposal submission, expert peer-group review, the sched-uling and carrying out of the granted experiment, subsequent data analysis, and the final publication of results. To date, it takes approximately more than 6 months between proposal acceptance and further data collection, and more than 1.5 years on average before data interpretation/publication of the collected data. More-over, correlations with modeling, databases, and artificial intel-ligence (AI) are usually limited to the very early (design of an experiment) or the very final (discussion about output parame-ters) stage of the linear sequential process. Finally, the realization and interpretation of one experiment usually implies decision-making operators, advanced human expertise, and manual oper-ations, because data acquisition and its subsequent analysis/interpretation is seldom automatized.

In order to progress beyond single-parameter and/or single-scale investigations, some synchrotron beamlines
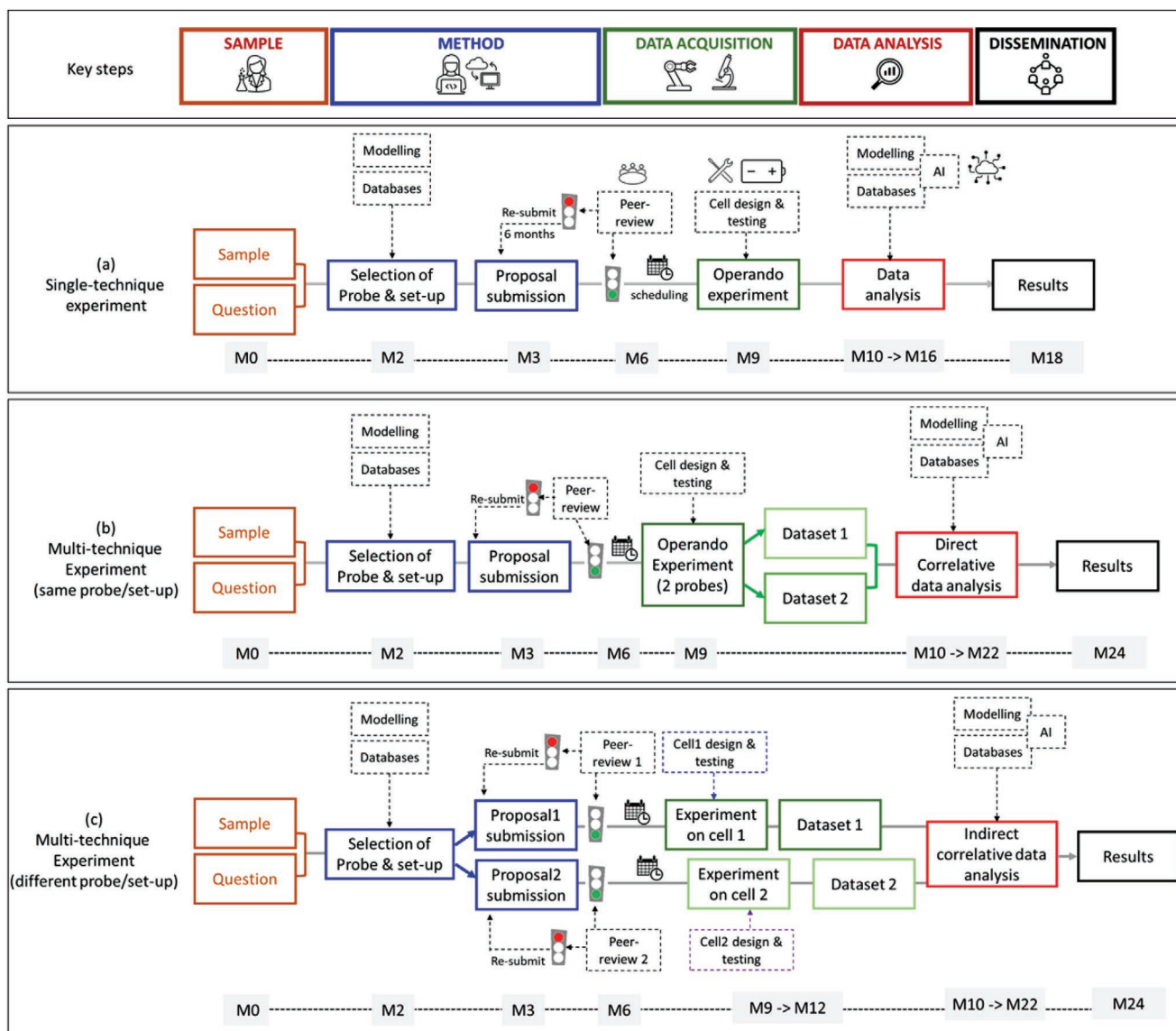
Figure 5. Current LSF experimental workflows based on the linear succession of key steps: sample, method, data acquisition, data analysis, and dissemination. a) Single-technique experiment aiming at characterizing one type of battery cell to obtain one type of information by performing one specific operando experiment. b) Progresses toward a multi-technique workflow enabled by multi-technique beamlines/instrumentation and subsequent direct correlative analysis or c) indirect correlative data analysis applied to datasets obtained on different beamlines/instruments. In all cases, modeling and databases are usually employed to decide/apply method and analysis steps. Advanced AI-techniques (ML, DL) are possibly employed to accelerate data analysis. The main time-limiting steps are the proposal submission/evaluation by peer-review, the scheduling of experiment at selected instrument(s), and the analysis of big data generated by operando measurements, as well as handling, storage, formatting, and analysis of multiple data sets for coupled experiments. The human operator is needed at all stages of the process to take decisions on sample environment/battery cell, probe/set-up conditions, raw data acquisition protocols, data pre-processing/analysis methods, extraction of output parameters, and finalization of results.

and neutron instruments offer the possibility of multi-probe characterizations, for example, to simultaneously measure XAS and XRD,[44] SAXS and WAXS,[52,53] SANS and lab-SAXS,[61] NCT and lab-XCT,[38] thus allowing access to co-registered, complementary data in a single-shot (e.g., both morphological and chemical information) and/or covering the multiple length-scales of interest (Figure 5b). However, as the situation stands today, most multi-technique studies generally rely on the sequential access to different instruments (Figure 5c). These experimental workflows are still subject to those bot-

tlenecks encountered in single-technique experiments. Additionally, the timeframe may even be extended due to the difficulty in developing multi-technique-compatible sample preparation procedures, coordinating access to several instruments, the collection/processing/storage of several datasets, and their subsequent correlative analysis – a process requiring relatively recent, non-trivial solutions and mostly limited to statistical and/or qualitative combinations. Therefore, the coupling/correlation and/or combination of LSF experiments remains uncommon, and multi-technique methodologies and

**ADVANCED
SCIENCE NEWS**
www.advancedsciencenews.com

**ADVANCED
ENERGY
MATERIALS**
www.advenergymat.de

workflows for correlative data acquisition and analysis are still in their infancy.

5. Toward an Integrated Correlative Characterization Approach

The importance for correlative characterization has been recognized in the domain of life sciences[90] where it is now extensively deployed. In the domain of material science, correlative characterization has received significant attention recently because of its capacity to offer insights into complex, inter-related phenomena such as the relationship between structural and/or morphological properties and material performance during operation. Some of the tools available to the scientific community were presented in the extensive review proposed by Robertson et al.[91] The capability of performing multiple characterizations, together with the possibility of implementing high-throughput material synthesis (one of the pillars of "materiomics"), together with a very mature concern by the community to develop adapted standards, contributed to the creation of a new paradigm in material discovery. Above and beyond space correlation, 4D methodologies were introduced, where time correlations formed the fourth dimension. "Correlative multifaceted characterizations", as defined by Burnett and Withers,[92] are shown as a special family of spatial/temporal correlated experiments and refer to complementary acquisitions of a physical phenomenon at the same region of interest, either simultaneously on a unique instrument (as in Figure 5b) or consequentially in the case of multi-instrument measurements (as in Figure 5c). This methodology, defined as being multimodal, is receiving widespread adoption in materials science. However, the field of battery research is less reactive and much work still needs to be done before correlative methods can be routinely implemented to characterize battery materials and devices by LSF techniques. Indeed, coordinated, quasi-simultaneous access to several beamlines/instruments is required, including complementary neutron and synchrotron measurements, to guarantee experimental optimization and to correlatively gather information on multi-length scales (structural, electronic & chemical properties, morphology, and more). Such correlative (multi-modal, multi-scale) characterization frameworks are currently foreseen, juxtaposing new methodologies with accelerated experimental timescales and faster science dissemination, corresponding to actual battery R&D lead-times.

The paradigm shift toward a robust correlative characterization approach in batteries requires novel types of workflows designed to tackle LSF-specific bottlenecks:

1) The linear sequence of actions extending over months/years to prepare, realize, and analyze a specific experiment, including the time-limited access to specific instruments,
2) The active presence of expert users at each step of data collection and analysis,
3) The availability of standardized LSF-compatible battery cells to perform operando correlative characterization,
4) The generation of big and diversely formatted data volumes,

5) The transfer of results to the research community and accelerated return-on-investment to battery R&Ds.

The automatization and standardization of multi-technique correlative experiments is fundamental to meeting these challenges. Accelerating 1) and 2) requires the implementation of modern tools such as active learning and DL/ML modules, as well as on-the-fly diagnostic and fast feed-back loops, ultimately enabling the on-line control of data acquisition and experimental set-up selection. Accelerating 2) and 4) requires expert databases/repositories, centralized platforms and apps, new software capable to handle multidimensional datasets and perform autonomous correlative data analysis. Accelerating 1) and 5) requires new access modes to enable fast, reactive, and flexible beamtime allocation, scheduling and use, ultimately leading to the coordination of multi-site experiments carried out on the same material/device and under the same operational conditions, which implies the development of standardized cell designs and operating procedures, as well as new infrastructures.

A novel type of integrated workflow is proposed in **Figure 6** for correlative (multi-modal, multi-technique) LSF-based research incorporating accelerators acting along the whole experimental chain. These include four key innovations which will be described in more detail in the next sections: 1) standardization of battery cells for multi-modal correlative operando characterization, 2) automated data acquisition systems and standardization of protocols and data management, 3) dynamic correlative analysis based on AI modules and intelligent batteries, and 4) new access modes to LSF, eventually with interoperable infrastructures.

5.1. Standardization of Cells for Correlative LSF Operando Characterizations

A key aspect of operando battery characterization is the development of beamline-compatible, reliable electrochemical cells as close as possible to commercial batteries; a task far from being routine and demanding significant advances to ensure data reliability, reproducibility, and fidelity. We can cite maintaining internal pressure for solid-state cells or respecting the ratio of electrode loading/electrolyte to active material (Li–S cells) as two instances. Of course, applying neutron/X-ray characterization techniques to commercial cells would wholly meet this criterion, but generally, customized cells are needed as a compromise between beamline/instrument requirements and electrochemical conditions, especially for long-term ageing studies. The development of bespoke cells is becoming even more critical for coupled and correlative experiments as reconfigurable and/or versatile, multi-techniques standardized designs are requested.

Since the 90s, a variety of casing, dimensions, and geometries have been adapted to neutron or synchrotron set-ups, specifically designed to investigate different categories of materials (solids, liquids, thin films). **Figure 7**a shows some of the cells developed during the last 10 years. Currently, there are very few cells compatible for more than one technique, or indeed for use with both neutrons to X-rays. Nevertheless, using the same cell on several beamlines would be an important step in achieving the goal of direct comparison of (operando) battery behavior by
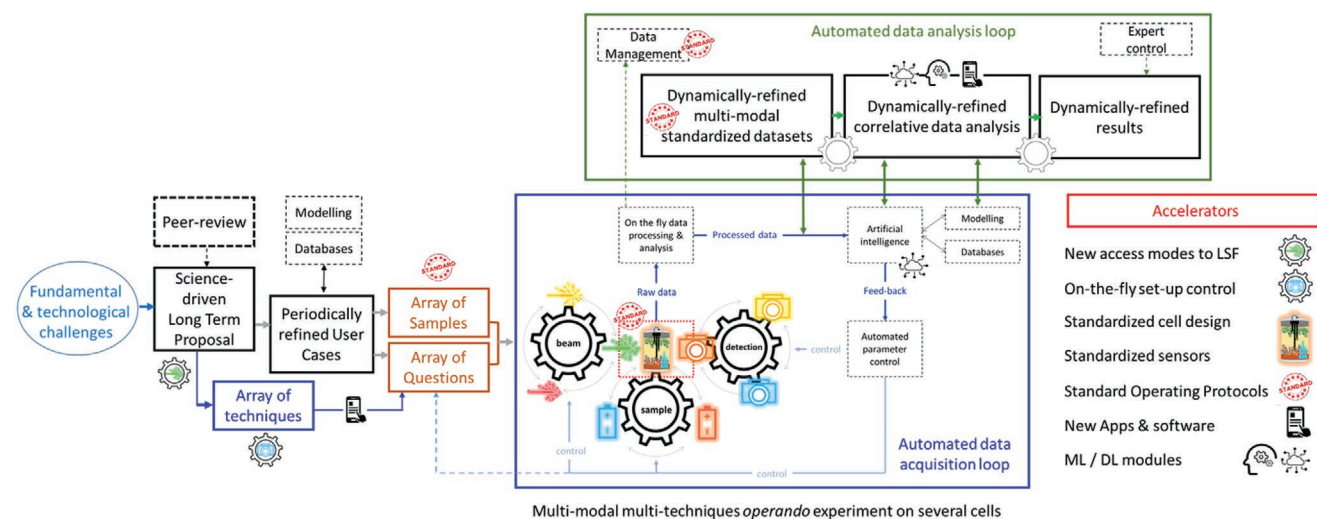
Figure 6. Multi-modal multi-technique correlative characterization workflow, where data acquisition (blue box) and analysis (green box) is accelerated by implementing on-the-fly monitoring, on-line data acquisition feed-back loops, dynamically-refined storage, and processing of standardized datasets by correlative analysis. The automated data acquisition loop allow controlling and modifying on request the beam characteristics and experimental conditions as well as the sample (change the region of interest in the probed battery, and/or move to next battery; ultimately, propose new materials combinations and robotically fabricate new cells). The workflow relies on the development and integration of accelerators applied during all key steps: from new access modes to LSF to new standards for battery & set-up protocols, apps, software, and ML/DL modules. The as-designed operando experiment provides high-throughput (multiple-sample data in fast mode) and/or high-fidelity data (selection of best conditions by automated loops for high-resolution / high-density mapping of selected parameters). The human expertise-driven decisions and actions are limited to the verification of automatisms and post-experiment analysis control.

providing chemical, electronic, structural, and morphological datasets acquired in the same conditions. Standardization of experimental cell designs is one of the principal challenges of the Battery 2030+/BIG-MAP project, together with standardization of data acquisition modes (including coordinated workflows) and (big) data analysis procedures. The BIG-MAP vision is to develop a modular, closed-loop infrastructure and methodology to bridge physical insights and data-driven approaches, by cohesively integrating machine learning, computer simulations, AI-orchestrated experiments, and synthesis, in order to accelerate battery materials discovery and optimization.[93] One key pillar of this vision is the development of a European multi-modal characterization platform for battery technology, including operando characterization at LSF, and thus ideally positioned for the coordination of multi-technique experiments to acquire and exploit multi-scale/multi-fidelity data. Included in this goal is making available multi-technique-compatible cells, for example, for coupling NI/SANS or XAS/XRD, as well as multi-modal compatible cells such as an imaging cell suitable for both neutron and synchrotron tomography (Figure 7b). At the 2030 horizon, highly versatile battery cells adaptable to a large array of beamlines and set-ups can be further envisioned – an example of this being the 2030-battery cell which would allow spectroscopic, scattering, imaging, and tomography experiments (Figure 7c).

5.2. Automated Data Acquisition and Autonomous, On-The-Fly Analysis

The foundation stone for implementing automated workflows in the field of batteries is the development of automated data acquisition and analysis. Both fields of computational data

and organic chemistry (e.g., pharmaceutics) have thrived due to the early introduction of machine learning capabilities and high-throughput automated testing, such as liquid NMR spectroscopy. However, materials science and battery materials/cells have yet to profit from their systematic implementation. Indeed, the complexity of the physical and chemical information required to exhaustively define battery materials throughout their entire life cycle is significantly greater than for either liquids or individual molecules.[105] To achieve automated workflows, the implementation of standards and protocols enabling high-throughput and high-fidelity data collection, as well as on-the-fly analysis, will be critical, requiring the development of innovative data management structures.

5.2.1. High-Throughput and High-Fidelity Data

A key challenge for LSF-based autonomous characterization is to combine the development of standardized experimental cells with the use of cell formats whose assembly can be automated for synchrotron and/or neutron testing. High throughput assembly and testing of battery electrolytes and battery interface properties has been demonstrated in different configurations, either through the use of standard plates[106] or scanning droplet configuration.[107] Similarly, automated coin cells assembly has also been demonstrated, although these are generally unsuitable for synchrotron or neutron testing. Hence, recent automated workflows using X-ray diffraction data for both laboratory and synchrotron X-ray sources[108] are difficultly transposable to the study of battery electrodes. Protocols for battery assembly previously defined for lab-scale cell formats[109] must be transposed to experimental LSF cells as those described in Figure 7. Common sample holders/changers
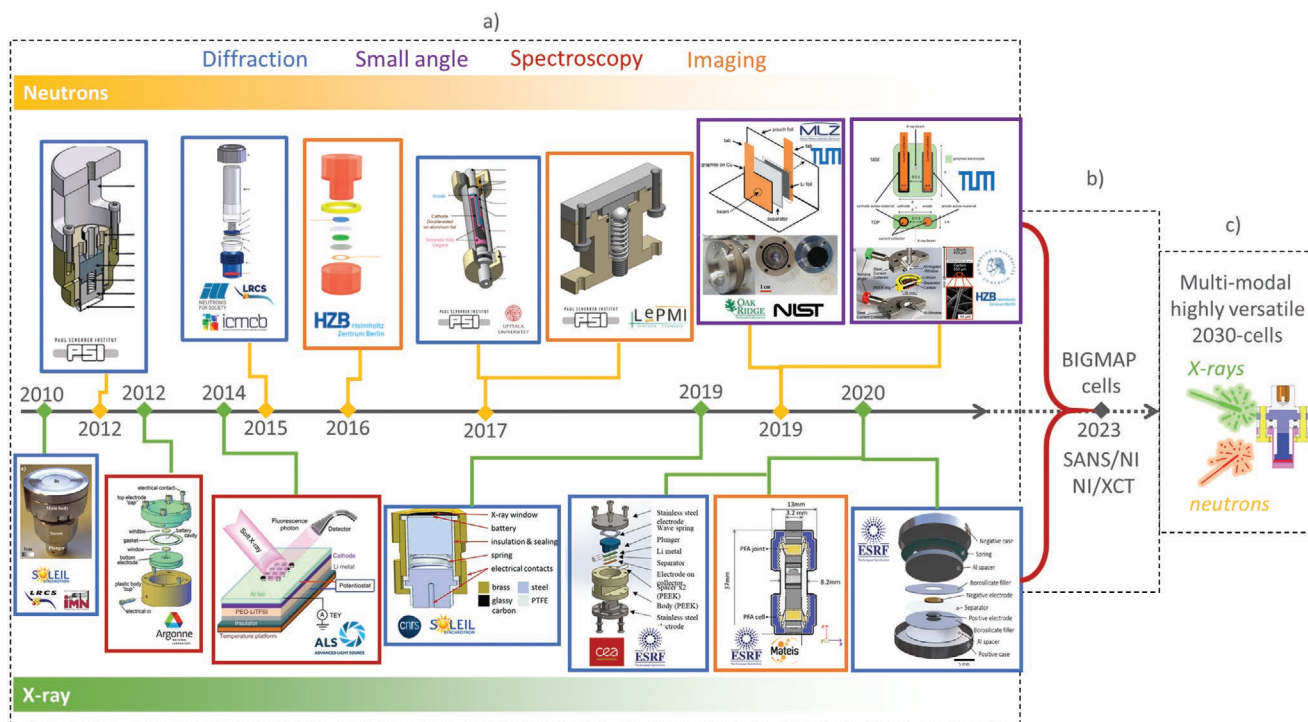
**ADVANCED
SCIENCE NEWS**

www.advancedsciencenews.com

**ADVANCED
ENERGY
MATERIALS**

www.advenergymat.de

Figure 7. a) Cells developed in the last 10 years for neutron (top) and synchrotron (bottom) characterizations, compatible with diffraction (blue squared boxes), small angle (purple), spectroscopy (red), and imaging (orange) techniques. Top side from left to right; neutron diffraction cell from PSI, Reproduced with permission.[36] Copyright 2013, Royal Society of Chemistry. Neutron diffraction cell from ILL/ICMCB/LRSC. Reproduced with permission.[94] Copyright 2013, Electrochemical Society. Imaging cell from HZB. Reproduced with permission.[95] Copyright 2019, Wiley and Sons. Neutron diffraction cell cylindrical neutron diffraction cell from PSI. Reproduced according to the terms of the CC-BY license.[96] Copyright 2018, The Authors. Neutron imaging cell from PSI/LEPMI. Small angle cell from TUM/MLZ, Reproduced according to the terms of the CC-BY license.[98] Copyright 2020, The Authors. Small angle cell from HZB/TUB. Reproduced with permission.[50] Copyright 2019, American Chemical Society. Reproduced with permission.[60] Copyright 2018, American Chemical Society. Bottom side from left to right; Leriche cell for diffraction, Reproduced with permission.[99] Copyright 2010, Electrochemical Society. Spectroscopy cell from Argonne. Reproduced with permission.[100] Copyright 2012, International Union of Crystallography. Spectroscopy cell from ALS. Reproduced with permission.[101] Copyright 2013, The Authors. Diffraction cell from Soleil, reproduced with permission.[102] Copyright 2019, International Union of Crystallography. Microdiffraction cell from CEA/ESRF cell, reproduced with permission.[25] Copyright 2021, Royal Society of Chemistry. Imaging cell from ESRF/Mateis, reproduced with permission.[103] Copyright 2021, American Chemical Society. Diffraction cell from ESRF, Reproduced with permission.[104] Copyright 2020, Royal Society of Chemistry. b) Progresses targeted within BIGMAP project to develop multi-techniques-compatible (NI/SANS) and/or multi-modal (NI/XCT) cells. c) Future developments at horizon 2030 for highly versatile cells compatible with an extended portfolio of X-rays and neutron tools.

and/or use of fiducial markers are crucial for data collection 1) across different types of probes / set-ups on the same battery and/or 2) across several batteries (Gear wheels in Figure 6). This fundamental attribute of the LSF workflow is common to other lab-scale multi-dataset methodologies, for instance multi-scale correlation microscopy, where the routine collection and manipulation of data on samples across multiple instruments necessitates controlled sample transfers and spatial references to enable the transfer of system coordinates.[92]

5.2.2. On-The-Fly Analysis and On-Line Control of Data Acquisition

Identifying and designing tasks that can be carried out without the need of an external operator must be at the forefront of the development of automated workflows. The implementation of automated data acquisition, when coupled with automated analysis, is a unique opportunity to develop better machine learning models, enabling the comparison of results from experimental and theoretical studies, as well as being crucial for future accelerated research. Integrating appropriate feedback loops, including extensive material

databases and advanced theoretical predictions, promises to profoundly change our use of synchrotron and neutron sources for battery research. By the real-time interpretation of results acquired during operando measurements, data acquisition conditions such as cycling protocols, energy/angle ranges, time/length resolutions, regions of interest, and so on, may be modified on-the-fly by a centralized AI to provide direct and fast access to required information, and adapt acquisition strategies/trajectories (Blue box in Figure 6). Recommendations for experimental refinements will be possible using the data obtained from on-line acquisition and analysis, thus dynamically refining the workflow toward ideal measurement conditions with respect to the sample, and/or (remotely) refining the sample material itself based on AI/ML analyses.

5.2.3. Innovative Data Management

Perhaps the main challenge that battery researchers face today for multimodal testing is the acquisition, registration, and handling of often bulky and pluriform (multi-layered multi-dimensional) datasets – all of which share a common reference

system. Appropriate software/methodology must be developed capable of handling such diverse and complex datasets. Dedicated data management methodologies, if possible generalized across the community,[110] are needed in order to treat these large datasets generated from advanced workflows. In this respect, a promising candidate is the CHADA method[111] using the MODA system developed by the European Material Characterisation Council (EMMC) and adaptative to three particular correlative workflows, that is, sequential, interactive, and coupled systems, respectively.

A prerequisite for automated data acquisition and on-the-fly analysis is the use of common standards for data management across the different facilities. While raw data generated within automated workflows should ideally be made available to the centralized AI, the large size of data generated at synchrotrons and neutrons often precludes transferring them to one common repository. Instead, a processing and pre-analysis step should be carried out, generating processed data in a standardized and readable format (blue/green boxes in Figure 6). Furthermore, successfully linking physical properties as obtained by neutron and synchrotron data to physical properties of battery materials necessitates that sufficient metadata are collected during the acquisition. Indeed, these metadata should include information pertinent to the measurement itself, as well as information regarding the battery materials, assembly, and cycling. Collecting metadata requires the use of an adequate online laboratory notebook using a common vocabulary for defining battery components as well as the characteristics of most of the LSF experimental techniques, that is, a so-called ontology.[112]

5.3. Multi-Modal Correlative Analysis and Intelligent Batteries

Characterization at LSF and subsequent data interpretation are intertwined topics at the center of accelerated materials discovery and which, due to the volume of data generated, will necessitate the development and application of novel AI strategies and in-line sensing to maximize their potential benefits to the battery research community.

5.3.1. Novel AI-Strategies

High-throughput instruments of course require brilliant beams coupled with advanced detectors in order to generate sufficiently large data sets for high-fidelity data, whilst minimizing acquisition times to remain economically viable. In the context of BIG-MAP, the possibility of generating and analyzing large amounts of high-fidelity data at acceptable costs will be fundamental during the initial AI/ML/DL training process. Physics- or machine-learning-based models can be used to interrogate whole datasets and/or select sub-sets to be analyzed preferentially in order to reconstruct global information, therefore saving time and enabling correlations not foreseen during the experiments. For instance, the 3D reconstruction and segmentation of tomographic data can be accelerated by reducing the number of slices and filling the gaps to obtain the full high-resolution mappings, without the need to exploit all acquired

slices, or indeed automatically modifying the acquisition protocol itself to select the appropriate amount of data needed. Combinations of coarse-scale specimen-mapping followed by high resolution mappings in selected regions save time and optimize scientific output. The development of "AI-based packages" capable to manipulate, visualize, and interrogate the multi-faceted, multi-scale datasets is required. For instance, the DRFAM3D software[113] employs a three-level classification, that is, "elements", "features", and "ensemble of features" that represent three different length scales. Each voxel contains, respectively both attributes from the input data along with output data obtained from analysis and modelling performed on the input data.[114]

Complementary methods include advanced coupling to modeling, for example, for analyzing spectroscopic or diffraction data using DFT calculations.[115] Also, the advent of statistical methodologies such as principal components analysis (PCA) for analysing operando XAS and transmission X-ray microscopy represents a unique opportunity to extend automated analysis to other LSF techniques relevant to batteries.[116]

5.3.2. In-Line Sensing

The concept of correlated characterization in the LSF world clearly coincide with the possibility of focusing extremely brilliant X-ray or neutron beams at micro- and nano-spots and combining complementary beams (X-rays, neutrons, but also ions, lasers, muons, electrons), therefore implementing mapping methodologies for multimodal analyses. However, acquiring multimodal mapping describing the structural and morphological properties of a material only gives a partial view of the overall picture. As stated in ref. [92], developing techniques capable of extracting mappings of material performance (mechanical or electrical) and correlating these with results obtained by advanced characterization in-lab and at LSF, would be an extremely powerful method in understanding the intrinsic phenomena involved in the battery dynamics. In this perspective, cells will include onboard, smart instrumentalization, thus enabling for the first time, the complete monitoring of individual battery behavior – obtained by employing a full-cycle, integrated workflow impacted by materials and electrochemistry.

All batteries, by their very nature, degrade with time, so understanding which factors are dominant in this ageing process is critical for developing solutions targeting long cycling lives. Information collected by internal sensors[117] and sent by optical fibers or Wi-Fi will be used to predict/identify malfunctions, and eventually employ internally injected "cure solutions" to regain optimal battery operations. Among the internal parameters of the battery to be monitored during LSF experiments, we can identify three main families: those with safety implications (e.g., the detection of gas accumulation inside the cell), those linked to the battery lifetime (temperature and pressure, Li concentration), and finally, a beam damage indicator for synchrotron X-rays (a combination of temperature and pressure could be implemented). To date, the few studies reporting on internal sensors and optical fibers describe systems which monitor local temperature fluctuation, but with no additional

**ADVANCED
SCIENCE NEWS**

www.advancedsciencenews.com

**ADVANCED
ENERGY
MATERIALS**

www.advenergymat.de

data sensor. Many other important parameters, taken from the above mentioned three categories, could be monitored at beamlines during operando measurements. For example, pressure sensors could be implemented in solid-state batteries, although care must be taken on correctly disposing sensors within the cell. In general, the internal positioning of an optical fiber/sensor may cause several physical modifications to the cell, leading to possible variations in local electrochemical response. Sensors placed to capture electrochemical activity transparently will therefore need to be developed. For instance, using the existing current collector, tuned to give additional information about local temperature, pH, pressure, Li concentration, and more, is a promising possible solution for internal, non-intrusive, multi-parameter monitoring. The development of such self-monitoring cells for experimental, and ultimately commercial purposes, coupled with suitably built-in, chemical curation mechanisms activated by the "intelligent" battery, will involve long-term, international cooperative projects, but nevertheless presents an obtainable vision of the technology's future.

5.4. New Access Modes and Infrastructures

The multi-modal automated and correlative experimental workflow proposed in Figure 6 implies a profound methodological change for both battery and LSF scientists, to provide the framework for integrating and accelerating all aspects of battery characterization and development, and to achieve the move toward efficient reduction of big datasets into meaningful output parameters. Accordingly, new modes of cooperation must be organized to stimulate fast exchange and interconnections between the various communities in battery R&D (academic researchers, materials developers, industrials, end-users), LSF expert users, LSF scientists, computer scientists, big data analysts; bringing together advances in computer science, informatics, robotics, manufacturing, sensors, materials science (including combinatorial synthesis), and characterization science (including lab scale and LSF).

5.4.1. New Access Modes at LSF

Clearly, the standard way of using LSF for complex, long-term, and strategic R&D challenges in the battery domain will need to evolve. As already mentioned, LSF provides access to their instruments via a proposal system, breaking down the access procedure into a series of time-consuming steps. Successive experiments or series of experiments using a variety of techniques on different instruments may include inherently procedural delays which, added together, can constitute a substantial timeline before final answers to complex scientific or technical problems can be given. For instance, in the case of multiple proposals to study new innovative materials on several instruments, peer-reviewing every individual request for access and analyzing in each case their potential scientific interest/impact without necessarily having all the elements needed to see "the bigger picture", may result in long lead-times incompatible with modern battery R&D. Also, battery research is carried out by a very large and diverse research community with a

very wide range of scientific and technical challenges. This, in turn, makes it difficult for LSF to select an optimized portfolio of experiments with maximum impact as there is currently no forum for exchanging within this specific research community itself. In this respect, LSF could serve as nucleation sites around which a given research community can assemble in order to foster a more structured approach for the use of the tools provided by the LSF. For the battery research community such a structured approach could include, for instance,

- repeated access for long-term monitoring of samples and processes –, for example, for studies of ageing and degradation with cycling,
- access to multiple instruments at more than one LSF with a single proposal –, for example, for multimodal characterization of electrochemical processes on a variety of electrode materials / battery cells,
- regular access based on long-term research programs instead of stand-alone experiments –, for example, for a structured R&D approach to advance the development of next-generation battery materials.

Some of these access modalities are already implemented on a small scale on a few instruments at some LSF. Block allocation group (BAG) and/or science-driven long-term proposals (LTP) could be adapted to groups working in battery materials with medium-term guaranteed access to beamlines. These mechanisms would enable enhanced flexibility and reactivity to simultaneously tackle an array of cross-sectorial scientific questions and probe an array of samples, for example, technological- and/or chemistry-expanded campaigns of measurements where several types of materials/batteries may be investigated in parallel and correlatively (Figure 6).

5.4.2. New Infrastructures

Expanding these modes of access to a larger portfolio of instruments, including those from several individual LSF (for example, at both neutron and synchrotron sources), would provide important and unique opportunities for a synchronized effort to solve R&D challenges. Integrating a large research community in such a structured approach could then provide justification for the creation of dedicated ancillary laboratories and tools at LSF, which could in turn develop into dedicated hubs for R&D in areas of high societal relevance. The advantage of such a European Battery Hub will be to gather diverse expert communities in order to establish the operational conditions and develop innovative workflows where the probes and set-ups, standardized smart cells, notebooks using common standards and protocols, toolkits for data storage, processing and analysis, and human resources are available and can be accessed/intertwined more efficiently. This would allow us to envision a transition from today's dispersed and isolated battery R&D activities to a future where battery characterization will be integrated, automated and unified (**Figure 8**); aiming at contributing to the fast-make, fast-data centric discovery, and manufacturing of new batteries.
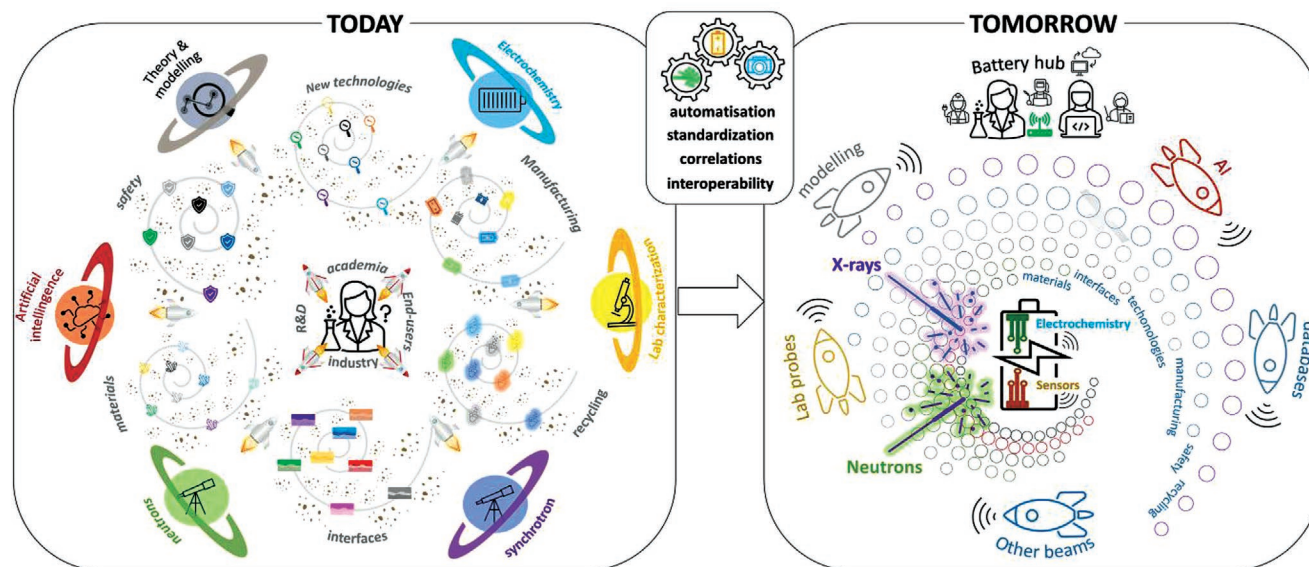
Figure 8. The paradigm shift in battery research: from today's dispersed and isolated R&D activities (left) to tomorrow's vision of a unified battery universe (right). Battery researchers have an array of tools available (multi-scale modeling, AI methods, electrochemical testing, lab- and LSF-characterization – planets in the battery system) with which to investigate generally individual aspects, for example, material development, new technologies, interface engineering, safety, manufacturing, recyclability – the many galaxies constituting the battery universe. Links and connections from a galaxy to another one from one planet to another are established, but iterations and correlations happen via step-by-step trials which are quite often non-related as everyone works separately in his/her own galaxy/planet. Novel workflows will enable new methodologies and infrastructures, permitting advanced cross-sectorial fertilization, hence enabling a centralized-framework for battery innovation. The creation of battery hubs will allow battery scientists, LSF scientists, computer-scientists, and engineers to cooperate and expand their ability to share knowledge and skills toward fast-make developments and innovations.

6. Conclusion

Developing future batteries demands accelerating materials' discovery grounded in the in-depth understanding of the electrochemical processes that dictate battery electrochemical performance and ageing. This is an incredible challenge given the range of relevant time and length scales and the variety of properties and processes at play during a battery's life cycle. Synchrotron and neutron techniques are crucial in this endeavor due to their ability to deeply penetrate matter during battery operation, providing invaluable insights into reaction mechanism in model-based batteries as well as fully commercial devices. Both spatial and time resolutions are crucial to determine the relationship between redox activity, structural evolution, and their distribution within the active materials that determines the fate of batteries. To reach a holistic understanding of battery processes, developments in the way experimental research are carried out, for example, improved and combined LSF setups, realistic and multi-experiment operando cells, as well as a paradigm shift in workflow and LSF beam-time access modes, are needed. The advent of fourth generation synchrotrons and high flux neutron spallation sources open exciting vistas in these directions. However, to correlatively gather information on multi-length scales (structural, electronic & chemical properties, morphology, etc.), we need to create new workflows for coordinated, quasi-simultaneous access to several beamlines/instruments, including complementary neutron & synchrotron measurements, and ideally using identical samples and cells. Ultimately, it is only by implementing battery characterization in an integrated, automatized and unified manner which will lead to a real transition from today's dispersed and isolated battery R&D activities. In this perspective, standardized beam-compatible smart batteries may be scrutinized simultaneously by various experimental probes – a process that will be dynamically refined through AI and modeling loops on an accelerated timeframe – thus yielding extended, multi-scale, multi-parameter output data directly. This integrated, AI-driven battery-management system (BMS) aims at providing high return-on-investment information to materials designers, battery makers, and indeed all players of the value chain – from synthesis to the assembling, testing & manufacturing of optimized cells and/or new technologies – and will radically reduce future battery design lead-times and costs. To reach these goals, access procedures and infrastructure at LSF will be required to evolve, accompanied by the creation of battery characterization hubs permitting advanced cross-sectorial fertilization, hence changing profoundly actual paradigms and enabling a centralized-framework for battery innovation.

Conflict of Interest

The authors declare no conflict of interest.

[1] a) P. P. R. M. L. Harks, F. M. Mulder, P. H. L. Notten, *J. Power Sources* **2015**, *288*, 92; b) H. Li, S. Guo, H. Zhou, *J. Energy Chem.* **2021**, *59*, 191; c) S.-M. Bak, Z. Shadike, R. Lin, X. Yu, X.-Q. Yang, *NPG Asia Mater.* **2018**, *10*, 563.

[2] D. Liu, Z. Shadike, R. Lin, K. Qian, H. Li, K. Li, S. Wang, Q. Yu, M. Liu, S. Ganapathy, X. Qin, Q.-H. Yang, M. Wagemaker, F. Kang, X.-Q. Yang, B. Li, *Adv. Mater.* **2019**, *31*, 1806620.

[3] a) X. Wu, S. Li, B. Yang, C. Wang, *Electrochem. Energy Rev.* **2019**, *2*, 467; b) Y. Wu, N. Liu, *Chem* **2018**, *4*, 438.

[4] a) K. Märker, C. Xu, C. P. Grey, *J. Am. Chem. Soc.* **2020**, *142*, 17447; b) A. I. Freytag, A. D. Pauric, S. A. Krachkovskiy, G. R. Goward, *J. Am. Chem. Soc.* **2019**, *141*, 13758.

[5] a) A. Vizintin, J. Bitenc, A. Kopač Lautar, K. Pirnat, J. Grdadolnik, J. Stare, A. Randon-Vitanova, R. Dominko, *Nat. Commun.* **2018**, *9*, 661; b) B. M. Koo, D. A. D. Corte, J.-N. Chazalviel, F. Maroun, M. Rosso, F. Ozanam, *Adv. Energy Mater.* **2018**, *8*, 1702568.

[6] a) J. Fawdon, J. Ihli, F. L. Mantia, M. Pasta, *Nat. Commun.* **2021**, *12*, 4053; b) P. Jehnichen, C. Korte, *Anal. Chem.* **2019**, *91*, 8054.

[7] D. Atkins, E. Ayerbe, A. Benayad, F. Capone, E. Capria, I. E. Castelli, I. Cekic-Laskovic, R. Ciria, L. Dudy, J. M. R. Edström, H. Li, J. M. G. Lastra, M. Leal De Souza, V. Meunier, M. Morcrette, H. Reichert, P. Simon, J.-P. Rueff, J. Sottmann, W. Wenzel, A. Grimaud, *Adv. Energy Mater.* **2021**, https://doi.org/10.1002/aenm.202102687.

[8] M. S. Whittingham, *Chem. Rev.* **2004**, *104*, 4271.

[9] a) N. Nitta, G. Yushin, *Part. Part. Syst. Charact.* **2014**, *31*, 317; b) M. T. McDowell, S. W. Lee, W. D. Nix, Y. Cui, *Adv. Mater.* **2013**, *25*, 4966.

[10] D. Lin, Y. Liu, Y. Cui, *Nat. Nanotechnol.* **2017**, *12*, 194.

[11] D. Aurbach, B. D. McCloskey, L. F. Nazar, P. G. Bruce, *Nat. Energy* **2016**, *1*, 16128.

[12] J. Cabana, L. Monconduit, D. Larcher, M. R. Palacín, *Adv. Mater.* **2010**, *22*, E170.

[13] A. Van der Ven, Z. Deng, S. Banerjee, S. P. Ong, *Chem. Rev.* **2020**, *120*, 6977.

[14] a) A. Van der Ven, K. Garikipati, S. Kim, M. Wagemaker, *J. Electrochem. Soc.* **2009**, *156*, A949; b) G. K. Singh, G. Ceder, M. Z. Bazant, *Electrochim. Acta* **2008**, *53*, 7599.

[15] A. Van der Ven, J. Bhattacharya, A. A. Belak, *Acc. Chem. Res.* **2013**, *46*, 1216.

[16] D. Aurbach, *J. Power Sources* **2000**, *89*, 206.

[17] J. B. Goodenough, Y. Kim, *Chem. Mater.* **2010**, *22*, 587.

[18] A. Van der Ven, M. Wagemaker, *Electrochem. Commun.* **2009**, *11*, 881.

[19] T. Sasaki, C. Villevieille, Y. Takeuchi, P. Novák, *Adv. Sci.* **2015**, *2*, 1500083.

[20] W. Dreyer, J. Jamnik, C. Guhlke, R. Huth, J. Moškon, M. Gaberšček, *Nat. Mater.* **2010**, *9*, 448.

[21] T. Sasaki, Y. Ukyo, P. Novák, *Nat. Mater.* **2013**, *12*, 569.

[22] F. C. Strobridge, B. Orvananos, M. Croft, H.-C. Yu, R. Robert, H. Liu, Z. Zhong, T. Connolley, M. Drakopoulos, K. Thornton, C. P. Grey, *Chem. Mater.* **2015**, *27*, 2374.

[23] X. Zhang, T. W. Verhallen, F. Labohm, M. Wagemaker, *Adv. Energy Mater.* **2015**, *5*, 1500498.

[24] V. K. Peterson, C. M. Papadakis, *IUCrJ* **2015**, *2*, 292.

[25] S. Tardif, N. Dufour, J.-F. Colin, G. Gébel, M. Burghammer, A. Johannes, S. Lyonnard, M. Chandesris, *J. Mater. Chem. A* **2021**, *9*, 4281.

[26] A. Brennhagen, C. Cavallo, D. Wragg, J. Sottmann, A. Y. Koposov, H. Fjellvåg, *Batteries Supercaps* **2021**, *4*, 1035.

[27] C. Xu, B. Sun, T. Gustafsson, K. Edström, D. Brandell, M. Hahlin, *J. Mater. Chem. A* **2014**, *2*, 7256.

[28] M. Ebner, F. Marone, M. Stampanoni, V. Wood, *Science* **2013**, *342*, 716.

[29] D. Bresser, M. Leclere, L. Bernard, P. Rannou, H. Mendil-Jakani, G.-T. Kim, T. Zinkevich, S. Indris, G. Gebel, S. Lyonnard, L. Picard, *ChemSusChem* **2021**, *14*, 490.

[30] L. C. Duda, K. Edström, *J. Electron Spectrosc. Relat. Phenom.* **2017**, *221*, 79.

[31] M. Wolf, B. M. May, J. Cabana, *Chem. Mater.* **2017**, *29*, 3347.

[32] C. Cao, H.-G. Steinrück, B. Shyam, M. F. Toney, *Adv. Mater. Interfaces* **2017**, *4*, 1700771.

[33] a) M. Fehse, C. J. Sahle, M. P. Hogan, C. Cavallari, E. M. Kelder, M. Alfredsson, A. Longo, *J. Phys. Chem. C* **2019**, *123*, 24396; b) T. Nonaka, H. Kawaura, Y. Makimura, Y. F. Nishimura, K. Dohmae, *J. Power Sources* **2019**, *419*, 203.

[34] V. Vanpeene, J. Villanova, A. King, B. Lestriez, E. Maire, L. Roué, *Adv. Energy Mater.* **2019**, *9*, 1803947.

[35] N. Paul, M. Wetjen, S. Busch, H. Gasteiger, R. Gilles, *J. Electrochem. Soc.* **2019**, *166*, A1051.

[36] V. A. Godbole, M. Hess, C. Villevieille, H. Kaiser, J.-F. Colin, P. Novak, *RSC Adv.* **2013**, *3*, 757.

[37] B.-K. Seidlhofer, B. Jerliu, M. Trapp, E. Hüger, S. Risse, R. Cubitt, H. Schmidt, R. Steitz, M. Ballauff, *ACS Nano* **2016**, *10*, 7458.

[38] R. F. Ziesche, T. Arlt, D. P. Finegan, T. M. M. Heenan, A. Tengattini, D. Baum, N. Kardjilov, H. Markötter, I. Manke, W. Kockelmann, D. J. L. Brett, P. R. Shearing, *Nat. Commun.* **2020**, *11*, 777.

[39] a) Y. Zhang, K. S. R. Chandran, H. Z. Bilheux, *J. Power Sources* **2018**, *376*, 125; b) J. P. Owejan, J. J. Gagliardo, S. J. Harris, H. Wang, D. S. Hussey, D. L. Jacobson, *Electrochim. Acta* **2012**, *66*, 94.

[40] T. W. Verhallen, S. Lv, M. Wagemaker, *Front. Energy Res.* **2018**, *6*, 62.

[41] a) K. I. S. Mongcopa, D. A. Gribble, W. S. Loo, M. Tyagi, S. A. Mullin, N. P. Balsara, *Macromolecules* **2020**, *53*, 2406; b) K. Mori, K. Enjuji, S. Murata, K. Shibata, Y. Kawakita, M. Yonemura, Y. Onodera, T. Fukunaga, *Phys. Rev. Appl.* **2015**, *4*, 054008.

[42] M. Bianchini, F. Fauth, N. Brisset, F. Weill, E. Suard, C. Masquelier, L. Croguennec, *Chem. Mater.* **2015**, *27*, 3009.

[43] K. M. Ø. Jensen, X. Yang, J. V. Laveda, W. G. Zeier, K. A. See, M. D. Michiel, B. C. Melot, S. A. Corr, S. J. L. Billinge, *J. Electrochem. Soc.* **2015**, *162*, A1310.

[44] P. Bleith, W. van Beek, H. Kaiser, P. Novak, C. Villevieille, *J. Phys. Chem. C* **2015**, *119*, 3466.

[45] G. Assat, D. Foix, C. Delacourt, A. Iadecola, R. Dedryvère, J.-M. Tarascon, *Nat. Commun.* **2017**, *8*, 2219.

[46] S. Lv, T. Verhallen, A. Vasileiadis, F. Ooms, Y. Xu, Z. Li, Z. Li, M. Wagemaker, *Nat. Commun.* **2018**, *9*, 2152.

[47] Z. Nie, P. McCormack, H. Z. Bilheux, J. C. Bilheux, J. P. Robinson, J. Nanda, G. M. Koenig, *J. Power Sources* **2019**, *419*, 127.

[48] L. Boulet-Roblin, D. Sheptyakov, P. Borel, C. Tessier, P. Novak, C. Villevieille, *J. Mater. Chem. A* **2017**, *5*, 25574.

[49] H. Kawaura, M. Harada, Y. Kondo, H. Kondo, Y. Suganuma, N. Takahashi, J. Sugiyama, Y. Seno, N. L. Yamada, *ACS Appl. Mater. Interfaces* **2016**, *8*, 9540.

[50] S. Risse, E. Härk, B. Kent, M. Ballauff, *ACS Nano* **2019**, *13*, 10233.

[51] a) A. V. Llewellyn, A. Matruglio, D. J. L. Brett, R. Jervis, P. R. Shearing, *Condens. Matter* **2020**, *5*, 75; b) W. Li, D. M. Lutz, L. Wang, K. J. Takeuchi, A. C. Marschilok, E. S. Takeuchi, *Joule* **2021**, *5*, 77.

[52] C. L. Berhaut, D. Z. Dominguez, P. Kumar, P.-H. Jouneau, W. Porcher, D. Aradilla, S. Tardif, S. Pouget, S. Lyonnard, *ACS Nano* **2019**, *13*, 11538.

[53] C. L. Berhaut, D. Z. Dominguez, D. Tomasi, C. Vincens, C. Haon, Y. Reynier, W. Porcher, N. Boudet, N. Blanc, G. A. Chahine, S. Tardif, S. Pouget, S. Lyonnard, *Energy Storage Mater.* **2020**, *29*, 190.

[54] A. Grenier, G. E. Kamm, Y. Li, H. Chung, Y. S. Meng, K. W. Chapman, *J. Am. Chem. Soc.* **2021**, *143*, 5763.

[55] Z. Feng, E. Sarnello, T. Li, L. Cheng, *J. Electrochem. Soc.* **2019**, *166*, A47.

[56] a) L. Aguilera, S. Xiong, J. Scheers, A. Matic, *J. Mol. Liq.* **2015**, *210*, 238; b) F. Lundin, L. Aguilera, H. W. Hansen, S. Lages, A. Labrador, K. Niss, B. Frick, A. Matic, *Phys. Chem. Chem. Phys.* **2021**, *23*, 13819.

[57] S. Seidlmayer, J. Hattendorff, I. Buchberger, L. Karge, H. A. Gasteiger, R. Gilles, *J. Electrochem. Soc.* **2015**, *162*, A3116.

[58] C. J. Jafta, C. A. Bridges, Y. Bai, L. Geng, B. P. Thapaliya, H. M. MeyerIII, R. Essehli, W. T. Heller, I. Belharouak, *ChemSusChem* **2020**, *13*, 3654.

[59] D. Saurel, J. Segalini, M. Jauregui, A. Pendashteh, B. Daffos, P. Simon, M. Casas-Cabanas, *Energy Storage Mater.* **2019**, *21*, 162.

[60] G. E. Möhl, E. Metwalli, P. Müller-Buschbaum, *ACS Energy Lett.* **2018**, *3*, 1525.

[61] E. Metwalli, K. Gotz, S. Lages, C. Bar, T. Zech, D. M. Noll, I. Schuldes, T. Schindler, A. Prihoda, H. Lang, J. Grasser, M. Jacques, L. Didier, A. Cyril, A. Martel, L. Porcar, T. Unruh, *J. Appl. Crystallogr.* **2020**, *53*, 722.

[62] M. K. Christensen, J. K. Mathiesen, S. B. Simonsen, P. Norby, *J. Mater. Chem. A* **2019**, *7*, 6459.

[63] D. P. Finegan, A. Vamvakeros, L. Cao, C. Tan, T. M. M. Heenan, S. R. Daemi, S. D. M. Jacques, A. M. Beale, M. Di Michiel, K. Smith, D. J. L. Brett, P. R. Shearing, C. Ban, *Nano Lett.* **2019**, *19*, 3811.

[64] L. Boulet-Roblin, P. Borel, D. Sheptyakov, C. Tessier, P. Novak, C. Villevieille, *J. Phys. Chem. C* **2016**, *120*, 17268.

[65] J. Conder, R. Bouchet, S. Trabesinger, C. Marino, L. Gubler, C. Villevieille, *Nat. Energy* **2017**, *2*, 17069.

[66] D. Petz, M. J. Mühlbauer, A. Schökel, K. Achterhold, F. Pfeiffer, T. Pirling, M. Hofmann, A. Senyshyn, *Batteries Supercaps* **2021**, *4*, 327.

[67] A. Senyshyn, M. J. Mühlbauer, K. Nikolowski, T. Pirling, H. Ehrenberg, *J. Power Sources* **2012**, *203*, 126.

[68] T. M. M. Heenan, C. Tan, J. Hack, D. J. L. Brett, P. R. Shearing, *Mater. Today* **2019**, *31*, 69.

[69] a) D. P. Finegan, A. Vamvakeros, C. Tan, T. M. M. Heenan, S. R. Daemi, N. Seitzman, M. Di Michiel, S. Jacques, A. M. Beale, D. J. L. Brett, P. R. Shearing, K. Smith, *Nat. Commun.* **2020**, *11*, 631; b) F. Tang, Z. Wu, C. Yang, M. Osenberg, A. Hilger, K. Dong, H. Markötter, I. Manke, F. Sun, L. Chen, G. Cui, *Small Methods* **2021**, *5*, 2100557; c) A. Senyshyn, M. J. Mühlbauer, O. Dolotko, M. Hofmann, T. Pirling, H. Ehrenberg, *J. Power Sources* **2014**, *245*, 678.

[70] a) Y. Nomura, K. Yamamoto, T. Hirayama, E. Igaki, K. Saitoh, *Microsc. Microanal.* **2019**, *25*, 1436; b) A. Banerjee, X. Wang, C. Fang, E. A. Wu, Y. S. Meng, *Chem. Rev.* **2020**, *120*, 6878; c) B. Koohbor, L. Sang, Ö. Ö. Çapraz, A. A. Gewirth, R. G. Nuzzo, S. R. White, N. R. Sottos, *J. Electrochemical Society* **2019**, *168*, 010516; d) X. Wu, J. Billaud, I. Jerjen, F. Marone, Y. Ishihara, M. Adachi, Y. Adachi, C. Villevieille, Y. Kato, *Adv. Energy Mater.* **2019**, *9*, 1901547.

[71] F. Sun, L. Duchêne, M. Osenberg, S. Risse, C. Yang, L. Chen, N. Chen, Y. Huang, A. Hilger, K. Dong, T. Arlt, C. Battaglia, A. Remhof, I. Manke, R. Chen, *Nano Energy* **2021**, *82*, 105762.

[72] C. Villevieille, M. Ebner, J. L. Gomez-Camer, F. Marone, P. Novak, V. Wood, *Adv. Mater.* **2015**, *27*, 1676.

[73] a) L. Lutz, W. Dachraoui, A. Demortière, L. R. Johnson, P. G. Bruce, A. Grimaud, J.-M. Tarascon, *Nano Lett.* **2018**, *18*, 1280; b) Z. Su, V. De Andrade, S. Cretu, Y. Yin, M. J. Wojcik, A. A. Franco, A. Demortière, *ACS Appl. Energy Mater.* **2020**, *3*, 4093.

[74] F. Sun, R. Gao, D. Zhou, M. Osenberg, K. Dong, N. Kardjilov, A. Hilger, H. Markötter, P. M. Bieker, X. Liu, I. Manke, *ACS Energy Lett.* **2019**, *4*, 306.

[75] G. Tonin, G. B. M. Vaughan, R. Bouchet, F. Alloin, M. Di Michiel, C. Barchasz, *J. Power Sources* **2020**, *468*, 228287.

[76] a) D. S. Eastwood, R. S. Bradley, F. Tariq, S. J. Cooper, O. O. Taiwo, J. Gelb, A. Merkle, D. J. L. Brett, N. P. Brandon, P. J. Withers, P. D. Lee, P. R. Shearing, *Nucl. Instrum. Methods Phys. Res., Sect. B* **2014**, *324*, 118; b) L. Li, Y. Xie, E. Maxey, R. Harder, *J. Synchrotron Radiat.* **2019**, *26*, 220.

[77] M. van Hulzen, F. G. B. Ooms, J. P. Wright, M. Wagemaker, *Front. Energy Res.* **2018**, *6*, 59.

[78] E. H. R. Tsai, J. Billaud, D. F. Sanchez, J. Ihli, M. Odstrčil, M. Holler, D. Grolimund, C. Villevieille, M. Guizar-Sicairos, *iScience* **2019**, *11*, 356.

[79] E. H. R. Tsai, J. Billaud, D. F. Sanchez, J. Ihli, M. Odstrcil, M. Holler, D. Grolimund, C. Villevieille, M. Guizar-Sicairos, *Iscience* **2019**, *11*, 356.

[80] X. Zhang, M. van Hulzen, D. P. Singh, A. Brownrigg, J. P. Wright, N. H. van Dijk, M. Wagemaker, *Nat. Commun.* **2015**, *6*, 8333.

[81] A. Ulvestad, A. Singer, H.-M. Cho, J. N. Clark, R. Harder, J. Maser, Y. S. Meng, O. G. Shpyrko, *Nano Lett.* **2014**, *14*, 5123.

[82] N. Ohmer, B. Fenk, D. Samuelis, C.-C. Chen, J. Maier, M. Weigand, E. Goering, G. Schütz, *Nat. Commun.* **2015**, *6*, 6045.

[83] J. F. M. Oudenhoven, F. Labohm, M. Mulder, R. A. H. Niessen, F. M. Mulder, P. H. L. Notten, *Adv. Mater.* **2011**, *23*, 4103.

[84] F. Linsenmann, M. Trunk, P. Rapp, L. Werner, R. Gernhäuser, R. Gilles, B. Märkisch, Z. Révay, H. A. Gasteiger, *J. Electrochem. Soc.* **2020**, *167*, 100554.

[85] a) F. Salvemini, F. Grazzi, N. Kardjilov, I. Manke, F. Civita, M. Zoppi, *Anal. Methods* **2015**, *7*, 271; b) L. Helfen, T. Baumbach, P. Mikulík, D. Kiel, P. Pernot, P. Cloetens, J. Baruchel, *Appl. Phys. Lett.* **2005**, *86*, 071915; c) L. Helfen, F. Xu, B. Schillinger, E. Calzada, I. Zanette, T. Weitkamp, T. Baumbach, *Nucl. Instrum. Methods Phys. Res., Sect. A* **2011**, *651*, 135.

[86] S. Tardif, E. Pavlenko, L. Quazuguel, M. Boniface, M. Maréchal, J.-S. Micha, L. Gonon, V. Mareau, G. Gebel, P. Bayle-Guillemaud, F. Rieutord, S. Lyonnard, *ACS Nano* **2017**, *11*, 11306.

[87] T. Vorauer, P. Kumar, C. L. Berhaut, F. F. Chamasemani, P.-H. Jouneau, D. Aradilla, S. Tardif, S. Pouget, B. Fuchsbichler, L. Helfen, S. Atalay, W. D. Widanage, S. Koller, S. Lyonnard, R. Brunner, *Commun. Chem.* **2020**, *3*, 141.

[88] S. Müller, M. Lippuner, M. Verezhak, V. De Andrade, F. De Carlo, V. Wood, *Adv. Energy Mater.* **2020**, *10*, 1904119.

[89] C. Zhao, T. Wada, V. De Andrade, D. Gürsoy, H. Kato, Y.-c. K. Chen-Wiegart, *Nano Energy* **2018**, *52*, 381.

[90] T. Ando, S. P. Bhamidimarri, N. Brending, H. Colin-York, L. Collinson, N. De Jonge, P. J. de Pablo, E. Debroye, C. Eggeling, C. Franck, M. Fritzsche, H. Gerritsen, B. N. G. Giepmans, K. Grunewald, J. Hofkens, J. P. Hoogenboom, K. P. F. Janssen, R. Kaufmann, J. Klumperman, N. Kurniawan, J. Kusch, N. Liv, V. Parekh, D. B. Peckys, F. Rehfeldt, D. C. Reutens, M. B. J. Roeffaers, T. Salditt, I. A. T. Schaap, U. S. Schwarz, et al., *J. Phys. D: Appl. Phys.* **2018**, *51*, 443001.

[91] I. M. Robertson, C. A. Schuh, J. S. Vetrano, N. D. Browning, D. P. Field, D. J. Jensen, M. K. Miller, I. Baker, D. C. Dunand, R. Dunin-Borkowski, B. Kabius, T. Kelly, S. Lozano-Perez, A. Misra, G. S. Rohrer, A. D. Rollett, M. L. Taheri, G. B. Thompson, M. Uchic, X.-L. Wang, G. Was, *J. Mater. Res.* **2011**, *26*, 1341.

[92] T. L. Burnett, P. J. Withers, *Nat. Mater.* **2019**, *18*, 1041.

[93] a) J. Amici, P. Asinari, E. Ayerbe, P. Barboux, P. Bayle-Guillemaud, R. J. Behm, M. Berecibar, E. Berg, A. Bhowmik, S. Bodoardo, I. E. Castelli, I. Cekic-Laskovic, R. Christensen, S. Clark, R. Diehm,

R. Dominko, M. Fichtner, A. A. Franco, A. Grimaud, N. Guillet, M. Hahlin, S. Hartmann, V. Heiries, K. Hermansson, A. Heuer, L. Jabbour, S. Jana, J. Kallo, A. Latz, H. Lorrmann, et al. *Adv. Energy Mater.*, https://doi.org/10.1002/aenm.202102785; b) A. Bhowmik, M. Berecibar, M. Casas-Cabanas, G. Csanyi, R. Dominko, K. Hermansson, M. R. Palacin, H. S. Stein, T. Vegge, *Adv. Energy Mater.* **2021**, https://doi.org/10.1002/aenm.202102698.

[94] M. Bianchini, J. B. Leriche, J. L. Laborier, L. Gendrin, E. Suard, L. Croguennec, C. Masquelier, *J. Electrochem. Soc.* **2013**, 160, A2176.

[95] K. Dong, H. Markötter, F. Sun, A. Hilger, N. Kardjilov, J. Banhart, I. Manke, *ChemSusChem* **2019**, 12, 261.

[96] L. Vitoux, M. Reichardt, S. Sallard, P. Novak, D. Sheptyakov, C. Villevieille, *Front. Energy Res.* **2018**, 6, 76.

[97] S. Sallard, J. Jasielec, M. Segwart, P. Trtik, P. Boillat, P. Peljo, C. Villevieille, Unpublished.

[98] J. Hattendorff, S. Seidlmayer, H. A. Gasteiger, R. Gilles, *J. Appl. Crystallogr.* **2020**, 53, 210.

[99] J. B. Leriche, S. Hamelet, J. Shu, M. Morcrette, C. Masquelier, G. Ouvrard, M. Zerrouki, P. Soudan, S. Belin, E. Elkaïm, F. Baudelet, *J. Electrochem. Soc.* **2010**, 157, A606.

[100] O. J. Borkiewicz, B. Shyam, K. M. Wiaderek, C. Kurtz, P. J. Chupas, K. W. Chapman, *J. Appl. Crystallogr.* **2012**, 45, 1261.

[101] X. Liu, D. Wang, G. Liu, V. Srinivasan, Z. Liu, Z. Hussain, W. Yang, *Nat. Commun.* **2013**, 4, 2568.

[102] J. Sottmann, V. Pralong, N. Barrier, C. Martin, *J. Appl. Crystallogr.* **2019**, 52, 485.

[103] Q. Lemarié, E. Maire, H. Idrissi, P.-X. Thivel, F. Alloin, L. Roué, *ACS Appl. Energy Mater.* **2020**, 3, 2422.

[104] D. P. Finegan, A. Quinn, D. S. Wragg, A. M. Colclasure, X. Lu, C. Tan, T. M. M. Heenan, R. Jervis, D. J. L. Brett, S. Das, T. Gao, D. A. Cogswell, M. Z. Bazant, M. Di Michiel, S. Checchia, P. R. Shearing, K. Smith, *Energy Environ. Sci.* **2020**, 13, 2570.

[105] H. S. Stein, J. M. Gregoire, *Chem. Sci.* **2019**, 10, 9640.

[106] B. D. Chambers, S. R. Taylor, M. W. Kendig, *Corrosion* **2005**, 61, 480.

[107] J. M. Gregoire, C. Xiang, X. Liu, M. Marcin, J. Jin, *Rev. Sci. Instrum.* **2013**, 84, 024102.

[108] L. Banko, P. M. Maffettone, D. Naujoks, D. Olds, A. Ludwig, *npj Comput. Mater.* **2021**, 7, 104.

[109] a) V. Murray, D. S. Hall, J. R. Dahn, *J. Electrochem. Soc.* **2019**, 166, A329; b) B. R. Long, S. G. Rinaldo, K. G. Gallagher, D. W. Dees, S. E. Trask, B. J. Polzin, A. N. Jansen, D. P. Abraham, I. Bloom, J. Bareño, J. R. Croy, *J. Electrochem. Soc.* **2016**, 163, A2999.

[110] I. E. Castelli, D. J. Arismendi-Arrieta, A. Bhowmik, I. Cekic-Laskovic, S. Clark, R. Dominko, E. Flores, J. Flowers, K. U. Frederiksen, J. Friis, A. Grimaud, K. V. Hansen, L. J. Hardwick, K. Hermansson, L. Königer, H. Lauritzen, F. L. Cras, H. Li, S. Lyonnard, H. Lorrmann, N. Marzari, L. Niedzicki, G. Pizzi, F. Rahmanian, H. Stein, M. Uhrin, W. Wenzel, M. Winter, C. Wölke, T. Vegge, *Batteries Supercaps* **2021**, 4, 1.

[111] N. Romanos, M. Kalogerini, E. P. Koumoulos, A. K. Morozinis, M. Sebastiani, C. Charitidis, *Mater. Today Commun.* **2019**, 20, 100541.

[112] S. Clark, J. Friis, F. L. Bleken, C. Andersen, E. Flores, M. Uhrin, S. Stier, M. Marcinek, A. Szczesna-Chrzan, M. Gaberscek, R. Palacin, *Adv. Energy Mater.* **2021**, https://doi.org/10.1002/aenm.202102702.

[113] M. A. Groeber, M. A. Jackson, *Integrating Materials and Manufacturing Innovation* **2014**, 3, 56.

[114] S. V. Kalinin, B. G. Sumpter, R. K. Archibald, *Nat. Mater.* **2015**, 14, 973.

[115] E. Flores, N. Mozhzhukhina, X. Li, P. Norby, A. Matic, T. Vegge, Unpublished.

[116] M. Fehse, A. Iadecola, M. T. Sougrati, P. Conti, M. Giorgetti, L. Stievano, *Energy Storage Mater.* **2019**, 18, 328.

[117] a) J. Huang, L. Albero Blanquer, J. Bonefacino, E. R. Logan, D. Alves Dalla Corte, C. Delacourt, B. M. Gallant, S. T. Boles, J. R. Dahn, H.-Y. Tam, J.-M. Tarascon, *Nat. Energy* **2020**, 5, 674; b) G. Han, J. Yan, Z. Guo, D. Greenwood, J. Marco, Y. Yu, *Renewable Sustainable Energy Rev.* **2021**, 150, 111514; c) A. Ghannoum, P. Nieva, *J. Energy Storage* **2020**, 28, 101233.
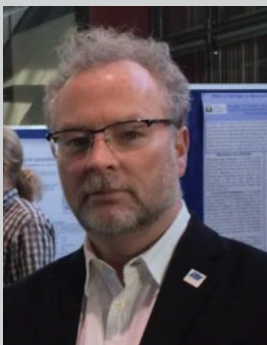
Duncan Atkins studied at Edinburgh University and Queen Mary's, University of London before moving to the Institut Laue Langevin, Grenoble France in 1990, where he was head of the High Flux Reactor Operation's Group until 2013 before integrating ILL's Industrial Liaison Group. He was instrumental in the design and construction of the neutron/x-ray tomography station D50/NeXT and is involved in promoting the full range of neutron experimental techniques available at the ILL to industry and academia, specifically in the domain of energy storage and battery research.

Ennio Capria is the Deputy Head of Business Development at the ESRF. In his research career he worked on the development of electrochemical nanobiosensors, nanocomposites and opto-electronic devices and particularly their characterisation with synchrotron light. At the ESRF, he is coordinating the participation of the ESRF in various collaborative initiative with industry, in particular on energy storage applications, additive manufacturing methods and nano-sciences. Since last year Ennio is Director of the Characterisation programme of the Technological Research Institute Nanoelec.
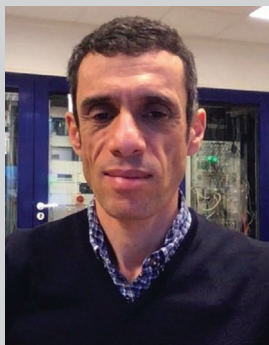
Jean-Pascal Rueff has received his Ph.D. in Condensed Matter Physics from University of Grenoble, France (1997). He is a CNRS Research Director and currently head of the GALAXIES beamline at the SOLEIL Synchrotron, France. His prime research focuses on investigating the electronic properties of complex materials including correlated electrons systems, 2D oxide heterostructures, and materials for batteries using x-ray spectroscopic techniques in the tender to hard x-ray range. This scientific activity also involves the development of novel instrumentation and methods using x-rays.

Claire Villevieille is currently CNRS research director (i.e. Full Prof) at the LEPMI laboratory in Grenoble, France. Her research is dedicated to the investigation of complex reaction mechanisms of battery systems such as Li-ion batteries and post Li-ion batteries by means of various operando techniques. Her research involves both, in-house devices as well as large facilities in France ERSF (Grenoble) and ILL (Grenoble), and, in Switzerland (SLS and SINQ). Her primary interests include solid state synthesis, electrochemical properties, and bulk–surface relationship of the various electrode materials.

Marnix Wagemaker received his Ph.D. in physics at Delft University Technology (2003) and since May 2017 is head of the section Storage of Electrochemical Energy and full professor at the Delft University of Technology in the Netherlands. His expertise's are battery materials and fundamental processes, and characterization of these, aiming at improved understanding and the development of next generation battery materials. Methods that he uses to study these include Neutron and X-ray scattering, solid state NMR, electrochemistry and density functional theory simulations.

Sandrine Lyonnard received her Ph.D. in Solid State Physics in 1997 from the University of Orsay, France. She is currently research director at CEA in Grenoble and deputy head of the Functional Materials Synthesis, Structure and Properties Group. She is a soft matter physicist specialized in the structure-transport interplay in nanostructured and ionic materials. Her research is dedicated to the development of scattering, imaging and spectroscopic operando techniques at Large Scale Facilities for the characterization of fuel cell and battery components and systems.